数理解析研究所講究録 1353 巻 2004 年 121-142



# Numerical Analysis of Thermal-Slip and Diffusion-Slip Flows of a Binary Mixture of Gases

Shigeru Takata (高田 滋), Shugo Yasuda (安田修悟), Shingo Kosuge (小菅真吾), Kazuo Aoki (青木一生)

Department of Aeronautics and Astronautics, Graduate School of Engineering,
Kyoto University, Kyoto 606-8501, Japan

**Abstract**

The thermal-slip (thermal-creep) and the diffusion-slip problems for a binary mixture of gases are investigated on the basis of the linearized Boltzmann equation for hard-sphere molecules with the diffuse reflection boundary condition. The problems are analyzed numerically by the finite-difference method incorporated with the numerical kernel method, which was first proposed by Sone et al. [Phys. Fluids A 1, 363 (1989)] for a single-component gas. As a result, the behavior of the mixture is clarified accurately not only at the level of the macroscopic variables but also at the level of the velocity distribution function. In addition, accurate formulas of the thermal-slip and the diffusion-slip coefficients for arbitrary values of the concentration of a component gas are constructed by the use of the Chebyshev polynomial approximation.

## 1 Introduction

When a gas is slightly rarefied or the Knudsen number is small, the overall behavior of the gas around solid bodies can be described by a system of fluid-dynamic-type equations with terms of gas rarefaction effect and slip (or jump) condition for the flow velocity (or the temperature). Here, the Knudsen number Kn is the ratio of the mean free path of the gas molecules to the reference length. The solution of the system is required to be corrected in a thin layer adjacent to the solid-body surface. The layer is of the thickness of a few mean free paths of the gas molecules and is called the Knudsen layer. The physical variables are subject to appreciable change there in the direction normal to the surface. These features were clarified by a systematic asymptotic analysis of the Boltzmann equation for small Knudsen numbers (Sone's asymptotic theory; see, for instance, Refs. [1–4]). The slip of flow (or the jump of temperature) and the Knudsen layer are considered as typical effects of gas rarefaction because they vanish when the continuum limit $\mathrm{Kn} \to 0$ is taken. This is a common understanding irrespective of whether the gas is pure or not.

In the meantime, Takata and Aoki [5] recently studied the steady behavior of a binary mixture of a vapor and a noncondensable gas around condensed phases of the vapor on the basis of kinetic theory. They carried out an asymptotic analysis of the Boltzmann equation for small Knudsen numbers and derived the fluid-dynamic type system which describes the behavior of the mixture in the situation where the Mach number of the flow is as small as the Knudsen number while the temperature variation of the condensed phase may be large. Contrary to the common understanding, the derived system shows that the slip condition for the flow velocity is necessary even in describing the behavior of the mixture in the continuum limit. This is an example of the recently discovered effect of gas rarefaction which remains at vanishing Knudsen number [6]; this phenomenon was termed the ghost effect (see Refs. [4, 7, 8] for details). The present paper is intended to provide accurate data of the slip boundary condition which causes the ghost effect in the mixture in a wide class of physical situations studied in Ref. [5].

The slip condition in the fluid-dynamic-type system derived in Ref. [5] can be obtained by the analysis of the thermal-slip (thermal-creep) [9] and the diffusion-slip [10] flows of a mixture over a plane wall. The former is the flow of the mixture induced along the wall by a uniform gradient of the wall temperature along its surface, and the latter is that induced along the wall by a uniform gradient of the concentration of a component gas along the surface. Many works have been devoted to the study of these flows (see, for instance, Refs. [10–26]). Most of the theoretical works were, however, limited to the analyses based on model equations or rough approximations such as the variational and the moment methods. Accurate analyses based on the original linearized Boltzmann equation were carried out only for the thermal-slip

flow of a single-component gas [16] and for the diffusion-slip flow of a binary mixture for several values of the concentration [22]. In order to complete the fluid-dynamic type system mentioned above, one needs the slip condition for arbitrary values of the concentration because the concentration generally varies along the boundary.

In the present paper, we investigate the thermal-slip and the diffusion-slip problems of a binary mixture of hard-sphere gases. We carry out an accurate numerical analysis based on the linearized Boltzmann equation and the diffuse reflection boundary condition for arbitrary values of the concentration of a component gas. The numerical method is a finite-difference method incorporated with the numerical kernel method, which was first proposed by Sone et al. [27] for a single-component gas and has been applied to various fundamental problems of rarefied gas dynamics [28–38]. The method was extended recently in Ref. [22] to a binary mixture of hard-sphere gases, prior to the present work. The paper is organized as follows. First the problems are formulated in Sec. 2. Then preliminary analysis is performed in Sec. 3, where the similarity solution and the expression of the collision integrals in terms of the integral kernel are introduced. The numerical method is developed on the basis of this expression in Sec. 4. The results are given and the discussions are made in Sec. 5.

# 2 Formulation of the Problem

## 2.1 Problem

We consider a semi-infinite expanse of a binary mixture of gases, gas A and gas B, over a plane wall. The wall is located at $X_1 = 0$, and the mixture occupies the region $X_1 > 0$, where $X_i$ is the rectangular coordinate system. We will investigate the steady behavior of the mixture in the following situations:
Problem I: The wall is kept at temperature $T_0 + \widetilde{C}_I X_2$ with $\widetilde{C}_I$ being a constant. Far from the wall, the state of the mixture is independent of $X_1$, the pressure of the mixture and the concentration of gas A (the number fraction of the molecules of gas A) are uniform, and the temperature of the mixture is the same as that of the wall $T_0 + \widetilde{C}_I X_2$, i.e., it has a uniform gradient in the $X_2$-direction.
Problem II: The wall is kept at a uniform temperature $T_0$. Far from the wall, the state of the mixture is independent of $X_1$, the pressure of the mixture is uniform, its temperature is also uniform and is the same as that of the wall $T_0$, and the concentration $X^A$ of gas A has a uniform gradient in the $X_2$-direction (thus the concentration $X^B$ of gas B has a uniform gradient of the same magnitude in the opposite direction, because $X^B = 1 - X^A$ by definition).
Problem I is called the thermal-slip problem, and problem II the diffusion-slip problem.

In what follows, the pressure of the mixture at infinity ($X_1 \to \infty$) is denoted by $p_0$. The concentration of gas A (or gas B) at infinity is denoted by $X_0^A$ (or $X_0^B$) in problem I, and by $X_0^A + \widetilde{C}_{II}^A X_2$ (or $X_0^B + \widetilde{C}_{II}^B X_2$) in problem II. Note that the relations $X_0^B = 1 - X_0^A$ and $\widetilde{C}_{II}^B = -\widetilde{C}_{II}^A$ hold by definition. The superscripts $\alpha$, $\beta$, and $\gamma$ are symbolically used to represent the gas species, i.e., $\alpha, \beta, \gamma = A, B$.

In the analysis, we make the following assumptions: (i) the molecules of gas $\alpha$ are hard spheres of mass $m^\alpha$ and diameter $d^\alpha$ and they collide elastically each other; (ii) the behavior of the mixture is described by the Boltzmann equation and the diffuse reflection condition for the reflected molecules on the wall; and (iii) the magnitude of the gradient of temperature in problem I and that of concentration in problem II are so small that the equations and boundary conditions can be linearized around the reference equilibrium state at rest with temperature $T_0$ and pressure $p_0$ of the mixture and concentration $X_0^\alpha$ of gas $\alpha$.

## 2.2 Basic equation and boundary condition

We first summarize the main notation used in the paper. The $n_0$ is the reference molecular number density of the mixture and is defined by $n_0 = p_0/kT_0$, where $k$ is Boltzmann's constant. The $\ell_0$ is the mean free path of the molecules in the equilibrium state at rest with the molecular number density $n_0$ and temperature $T_0$ when gas B is absent (i.e., $\ell_0 = 1/[\sqrt{2}\pi(d^A)^2 n_0]$). The $x_i$ is the nondimensional coordinate system defined by $x_i = X_i \ell_0^{-1}(\sqrt{\pi}/2)^{-1}$. The $(2kT_0/m^A)^{1/2}\zeta_i$ [or $(2kT_0/m^A)^{1/2}\zeta$] is the molecular velocity, $n_0(2kT_0/m^A)^{-3/2}(X_0^\alpha + \phi^\alpha)E^\alpha$ is the velocity distribution function of the molecules of gas $\alpha$, where $E^\alpha(\boldsymbol{\zeta}) = (\hat{m}^\alpha/\pi)^{3/2}\exp(-\hat{m}^\alpha|\boldsymbol{\zeta}|^2)$ with $\hat{m}^\alpha = m^\alpha/m^A$, and $\hat{d}^\alpha = d^\alpha/d^A$. The molecular number density, density, pressure, temperature, flow velocity, stress tensor, and heat-flow vector of gas $\alpha$

are denoted, respectively, by $n_0(X_0^\alpha+N^\alpha)$, $n_0 m^A(\hat{m}^\alpha X_0^\alpha+\omega^\alpha)$, $p_0(X_0^\alpha+P^\alpha)$, $T_0(1+\tau^\alpha)$, $(2kT_0/m^A)^{1/2}u_i^\alpha$, $p_0(X_0^\alpha\delta_{ij}+P_{ij}^\alpha)$, and $p_0(2kT_0/m^A)^{1/2}Q_i^\alpha$, where $\delta_{ij}$ is Kronecker's delta. Those of the mixture are denoted by $n_0(1+N)$, $n_0 m^A(\sum_{\beta=A,B}\hat{m}^\beta X_0^\beta+\omega)$, $p_0(1+P)$, $T_0(1+\tau)$, $(2kT_0/m^A)^{1/2}u_i$, $p_0(\delta_{ij}+P_{ij})$, and $p_0(2kT_0/m^A)^{1/2}Q_i$.

The linearized Boltzmann equation in the present case ($\partial/\partial t=\partial/\partial x_3=0$) is written as [39–41]

$$\zeta_1\frac{\partial\phi^\alpha}{\partial x_1}+\zeta_2\frac{\partial\phi^\alpha}{\partial x_2}=\sum_{\beta=A,B}K^{\beta\alpha}\tilde{L}^{\beta\alpha}(X_0^\alpha\phi^\beta,X_0^\beta\phi^\alpha), \tag{1}$$

where $\tilde{L}^{\beta\alpha}$ is the linearized collision integral defined by

$$\tilde{L}^{\beta\alpha}(f,g)=\frac{1}{4\sqrt{2\pi}}\int[f(\boldsymbol{\zeta}_*')-f(\boldsymbol{\zeta}_*)+g(\boldsymbol{\zeta}')-g(\boldsymbol{\zeta})]E^\beta(\boldsymbol{\zeta}_*)|\boldsymbol{e}\cdot\hat{\boldsymbol{V}}|d\Omega(\boldsymbol{e})d^3\boldsymbol{\zeta}_*, \tag{2}$$

with

$$\boldsymbol{\zeta}'=\boldsymbol{\zeta}+\frac{\hat{\mu}^{\beta\alpha}}{\hat{m}^\alpha}(\boldsymbol{e}\cdot\hat{\boldsymbol{V}})\boldsymbol{e},\quad \boldsymbol{\zeta}_*'=\boldsymbol{\zeta}_*-\frac{\hat{\mu}^{\beta\alpha}}{\hat{m}^\beta}(\boldsymbol{e}\cdot\hat{\boldsymbol{V}})\boldsymbol{e}, \tag{3a}$$

$$\hat{\boldsymbol{V}}=\boldsymbol{\zeta}_*-\boldsymbol{\zeta},\quad d^3\boldsymbol{\zeta}_*=d\zeta_{*1}d\zeta_{*2}d\zeta_{*3}, \tag{3b}$$

$$K^{\beta\alpha}=(\frac{\hat{d}^\alpha+\hat{d}^\beta}{2})^2,\quad \hat{\mu}^{\beta\alpha}=\frac{2\hat{m}^\alpha\hat{m}^\beta}{\hat{m}^\alpha+\hat{m}^\beta}. \tag{3c}$$

Here $\boldsymbol{e}$ is a unit vector, $\boldsymbol{\zeta}_*$ the variable of integration corresponding to $\boldsymbol{\zeta}$, and $d\Omega(\boldsymbol{e})$ the solid angle element in the direction of $\boldsymbol{e}$. The integration in Eq. (2) is carried out over the whole space of $\boldsymbol{\zeta}_*$ and over the all directions of $\boldsymbol{e}$.

The diffuse reflection condition on the wall ($x_1=0$) is written as

$$\phi^\alpha=c_I X_0^\alpha(\hat{m}^\alpha\zeta_j^2-2)x_2-2(\pi\hat{m}^\alpha)^{1/2}\int_{\zeta_1<0}\zeta_1\phi^\alpha E^\alpha d^3\boldsymbol{\zeta},\quad \zeta_1>0, \tag{4a}$$

for problem I (thermal slip), and

$$\phi^\alpha=-2(\pi\hat{m}^\alpha)^{1/2}\int_{\zeta_1<0}\zeta_1\phi^\alpha E^\alpha d^3\boldsymbol{\zeta},\quad \zeta_1>0, \tag{4b}$$

for problem II (diffusion slip). Here $c_I$ is the dimensionless gradient of the wall temperature defined by

$$c_I=\frac{\sqrt{\pi}}{2}\ell_0\frac{\tilde{C}_I}{T_0}.$$

Incidentally, for later use, we also define the dimensionless concentration gradient $c_{II}$ of gas A away from the wall by

$$c_{II}=\frac{\sqrt{\pi}}{2}\ell_0\tilde{C}_{II}^A.$$

The macroscopic variables $N^\alpha$, $\omega^\alpha$, $u_i^\alpha$, etc. of gas $\alpha$ are written in terms of $\phi^\alpha$ as

$$\begin{aligned}
N^\alpha&=\int\phi^\alpha E^\alpha d^3\boldsymbol{\zeta},\\
\omega^\alpha&=\hat{m}^\alpha\int\phi^\alpha E^\alpha d^3\boldsymbol{\zeta}(=\hat{m}^\alpha N^\alpha),\\
u_i^\alpha&=\frac{1}{X_0^\alpha}\int\zeta_i\phi^\alpha E^\alpha d^3\boldsymbol{\zeta},\\
\tau^\alpha&=\frac{2}{3}\frac{1}{X_0^\alpha}\int(\hat{m}^\alpha\zeta_j^2-\frac{3}{2})\phi^\alpha E^\alpha d^3\boldsymbol{\zeta},\\
P^\alpha&=\frac{2}{3}\hat{m}^\alpha\int\zeta_j^2\phi^\alpha E^\alpha d^3\boldsymbol{\zeta}(=N^\alpha+X_0^\alpha\tau^\alpha),\\
P_{ij}^\alpha&=2\hat{m}^\alpha\int\zeta_i\zeta_j\phi^\alpha E^\alpha d^3\boldsymbol{\zeta},\\
Q_i^\alpha&=\hat{m}^\alpha\int\zeta_i\zeta_j^2\phi^\alpha E^\alpha d^3\boldsymbol{\zeta}-\frac{5}{2}X_0^\alpha u_i^\alpha.
\end{aligned} \tag{5}$$

Here and henceforth, unless otherwise stated, the integration with respect to $\boldsymbol{\zeta}$ is performed over its whole space. The macroscopic variables of the mixture are expressed in terms of those of component gases as

$$\begin{aligned} &N = \sum_{\beta=A,B} N^\beta, \quad \omega = \sum_{\beta=A,B} \omega^\beta, \quad u_i = (\sum_{\beta=A,B} \hat{m}^\beta X_0^\beta u_i^\beta)/(\sum_{\beta=A,B} \hat{m}^\beta X_0^\beta), \\ &\tau = \sum_{\beta=A,B} X_0^\beta \tau^\beta, \quad P = \sum_{\beta=A,B} P^\beta, \quad P_{ij} = \sum_{\beta=A,B} P_{ij}^\beta, \quad Q_i = \sum_{\beta=A,B} [Q_i^\beta - \frac{5}{2} X_0^\beta (u_i - u_i^\beta)]. \end{aligned} \tag{6}$$

If we denote by $(X_0^\alpha + \chi^\alpha)$ the concentration of gas $\alpha$, $\chi^\alpha$ is expressed as

$$\chi^\alpha = N^\alpha - X_0^\alpha N. \tag{7}$$

Note that $\chi^A = -\chi^B$ because of the relations $N = N^A + N^B$ and $X_0^A + X_0^B = 1$.

# 3 Preliminary Analysis

## 3.1 Asymptotic solution away from the wall

Let us consider the function

$$\phi_{asy}^\alpha = X_0^\alpha [(\hat{m}^\alpha \zeta^2 - \frac{5}{2}) x_2 + 2\hat{m}^\alpha b_I \zeta_2 - \zeta_2 A^\alpha(\zeta)], \tag{8a}$$

for problem I and

$$\phi_{asy}^\alpha = (\delta_{\alpha A} - \delta_{\alpha B}) x_2 + 2\hat{m}^\alpha X_0^\alpha b_{II} \zeta_2 - X_0^\alpha \zeta_2 [D^{(A)\alpha}(\zeta) - D^{(B)\alpha}(\zeta)], \tag{8b}$$

for problem II, where $\zeta = |\boldsymbol{\zeta}| = \sqrt{\zeta_j^2}$, $\delta_{AA} = \delta_{BB} = 1$ and $\delta_{AB} = \delta_{BA} = 0$. Here $b_I$ and $b_{II}$ are undetermined constants, and the functions $A^\alpha$, $D^{(A)\alpha}$, and $D^{(B)\alpha}$ are the solutions of the following integral equations [40–42]:

$$\begin{aligned} &\sum_{\beta=A,B} K^{\beta\alpha} X_0^\beta \tilde{L}^{\beta\alpha}(\zeta_i A^\beta, \zeta_i A^\alpha) = -\zeta_i (\hat{m}^\alpha \zeta^2 - \frac{5}{2}), \\ &\text{subsidiary condition: } \sum_{\beta=A,B} \hat{m}^\beta X_0^\beta \int_0^\infty \zeta^4 A^\beta E^\beta d\zeta = 0, \end{aligned} \tag{9a}$$

and

$$\begin{aligned} &\sum_{\beta=A,B} K^{\beta\alpha} X_0^\alpha X_0^\beta \tilde{L}^{\beta\alpha}(\zeta_i D^{(\gamma)\beta}, \zeta_i D^{(\gamma)\alpha}) = -\zeta_i \left(\delta_{\alpha\gamma} - \frac{\hat{m}^\alpha X_0^\alpha}{\sum_{\beta=A,B} \hat{m}^\beta X_0^\beta}\right), \\ &\text{subsidiary condition: } \sum_{\beta=A,B} \hat{m}^\beta X_0^\beta \int_0^\infty \zeta^4 D^{(\alpha)\beta} E^\beta d\zeta = 0. \end{aligned} \tag{9b}$$

The function $\phi_{asy}^\alpha$ satisfies the Boltzmann equation (1). The corresponding macroscopic variables take the following form: for $\phi_{asy}^\alpha$ in Eq. (8a),

$$\begin{aligned} &N^\alpha = -X_0^\alpha x_2, \quad \omega^\alpha = -\hat{m}^\alpha X_0^\alpha x_2, \quad \tau^\alpha = x_2, \quad \chi^\alpha = P^\alpha = P_{ij}^\alpha = 0, \\ &u_i^\alpha = (b_I - \hat{D}_{T\alpha}) \delta_{i2}, \quad Q_i^\alpha = -\hat{\lambda}^{\alpha\prime} X_0^\alpha \delta_{i2}, \\ &N = -x_2, \quad \omega = -(\hat{m}^A X_0^A + \hat{m}^B X_0^B) x_2, \quad \tau = x_2, \quad P = P_{ij} = 0, \\ &u_i = b_I \delta_{i2}, \quad Q_i = -[\hat{\lambda}' + \frac{5}{2}(X_0^A \hat{D}_{TA} + X_0^B \hat{D}_{TB})] \delta_{i2}, \end{aligned} \tag{10a}$$

and for $\phi^\alpha_{asy}$ in Eq. (8b),

$$N^\alpha = P^\alpha = \chi^\alpha = (\delta_{\alpha A} - \delta_{\alpha B})x_2, \quad \omega^\alpha = \hat{m}^\alpha(\delta_{\alpha A} - \delta_{\alpha B})x_2, \quad \tau^\alpha = 0,$$
$$u_i^\alpha = (b_{II} - \hat{\Delta}_{\alpha A} + \hat{\Delta}_{\alpha B})\delta_{i2}, \quad P_{ij}^\alpha = (\delta_{\alpha A} - \delta_{\alpha B})x_2\delta_{ij}, \quad Q_i^\alpha = -X_0^\alpha(\hat{\Gamma}_D^{(A)\alpha} - \hat{\Gamma}_D^{(B)\alpha})\delta_{i2},$$
$$\omega = (\hat{m}^A - \hat{m}^B)x_2, \quad N = P = \tau = P_{ij} = 0, \quad u_i = b_{II}\delta_{i2}, \tag{10b}$$
$$Q_i = -[(\hat{D}_{TA} - \hat{D}_{TB}) + \frac{5}{2}\sum_{\beta=A,B} X_0^\beta(\hat{\Delta}_{\beta A} - \hat{\Delta}_{\beta B})]\delta_{i2}.$$

Here $\hat{\lambda}^{\alpha\prime}$, $\hat{\Delta}_{\alpha\beta}$, $\hat{D}_{T\alpha}$, $\hat{\Gamma}_D^{(\alpha)\beta}$, and $\hat{\lambda}'$ are functions of $X_0^A$, $\hat{m}^B$, and $\hat{d}^B$ and are related to the transport coefficients (see the Appendix A).

It is seen from the form of $P$, $\tau$, and $\chi^\alpha$ in Eq. (10a) that $\phi^\alpha_{asy}$ of (8a) multiplied by $c_I$ is the solution describing the state at infinity of problem I. Similarly, it is seen from the form of $P$, $\tau$, and $\chi^\alpha$ in Eq. (10b) that $\phi^\alpha_{asy}$ of (8b) multiplied by $c_{II}$ is the solution describing the state at infinity of problem II.

The asymptotic solution $c_I\phi^\alpha_{asy}$ or $c_{II}\phi^\alpha_{asy}$ is seen to represent the state of the mixture described by the fluid-dynamic equation. Therefore we call $c_I\phi^\alpha_{asy}$ or $c_{II}\phi^\alpha_{asy}$ the fluid-dynamic solution.

## 3.2 Knudsen-layer problems

Let us now seek the solution of problems I and II in the form

$$\phi^\alpha = c[\phi^\alpha_{asy} + \phi^\alpha_K(x_1, \zeta_i)], \tag{11}$$

where $c = c_I$ for problem I and $c = c_{II}$ for problem II. Substituting Eq. (11) into Eqs. (1) and (4a) or (4b) and taking into account that $\phi^\alpha_{asy}$ satisfies the condition at infinity, we obtain the following equation and boundary condition for $\phi^\alpha_K$:

$$\zeta_1\frac{\partial\phi^\alpha_K}{\partial x_1} = \sum_{\beta=A,B} K^{\beta\alpha}\tilde{L}^{\beta\alpha}(X_0^\alpha\phi_K^\beta, X_0^\beta\phi_K^\alpha), \tag{12}$$

$$\phi^\alpha_K = -2\hat{m}^\alpha X_0^\alpha b_I\zeta_2 + X_0^\alpha\zeta_2 A^\alpha(\zeta) - 2(\pi\hat{m}^\alpha)^{1/2}\int_{\zeta_1<0}\zeta_1\phi^\alpha_K E^\alpha d^3\boldsymbol{\zeta},$$
$$\zeta_1 > 0, \quad x_1 = 0 \quad \text{(problem I)}, \tag{13a}$$

$$\phi^\alpha_K = -2\hat{m}^\alpha X_0^\alpha b_{II}\zeta_2 + X_0^\alpha\zeta_2[D^{(A)\alpha}(\zeta) - D^{(B)\alpha}(\zeta)] - 2(\pi\hat{m}^\alpha)^{1/2}\int_{\zeta_1<0}\zeta_1\phi^\alpha_K E^\alpha d^3\boldsymbol{\zeta},$$
$$\zeta_1 > 0, \quad x_1 = 0 \quad \text{(problem II)}, \tag{13b}$$

$$\phi^\alpha_K \to 0, \qquad \text{as} \quad x_1 \to \infty. \tag{14}$$

We call the half-space problem (12), (13a), and (14) the Knudsen-layer problem for the thermal slip and the problem (12), (13b), and (14) that for the diffusion slip. For each problem, there is a unique solution $\phi^\alpha_K$ if and only if the constant $b_I$ or $b_{II}$ takes a special value, and $\phi^\alpha_K$ decays exponentially as $x_1 \to \infty$. This is a consequence of the existence and uniqueness theorem for the Knudsen-layer problem for a binary mixture of hard-sphere gases, which was proved recently in Ref. [43]. The theorem is the extension of that for a single-component gas first conjectured by Grad [44] and proved later for various molecular models [45–49]. In this way the constants $b_I$ and $b_{II}$ in the fluid-dynamic solutions, $c_I\phi^\alpha_{asy}$ and $c_{II}\phi^\alpha_{asy}$, are determined by the analysis of the Knudsen-layer problem. It is seen from the expression of $u_i$ in Eqs. (10a) and (10b) that $b_I$ or $b_{II}$ is the flow velocity of the mixture away from the wall when $c_I = 1$ or $c_{II} = 1$.

Since $\hat{m}^A = \hat{d}^A = 1$ and $X_0^A + X_0^B = 1$, both problems are characterized by the three parameters,

$$\hat{m}^B \ (\text{or } m^B/m^A), \quad \hat{d}^B \ (\text{or } d^B/d^A), \quad X_0^A.$$

Multiplying Eq. (12) by $\hat{m}^\alpha\zeta_2 E^\alpha$ for $\alpha = A, B$, adding the resulting equations, and taking into account the condition (14), one obtains the relation

$$\sum_{\beta=A,B}\hat{m}^\beta\int\zeta_1\zeta_2\phi^\beta_K E^\beta d^3\boldsymbol{\zeta} = 0. \tag{15}$$

This is the momentum conservation law in the $x_2$-direction.

### 3.3 Similarity solution and macroscopic variables

Let us assume that $\phi_K^\alpha$ is of the form

$$\phi_K^\alpha = (\zeta_2/\zeta_\rho)\Phi^\alpha(x_1, \zeta_1, \zeta_\rho), \tag{16}$$

where $\zeta_\rho = \sqrt{\zeta_2^2 + \zeta_3^2}$. This $\phi_K^\alpha$ is compatible with Eqs. (12)–(14), which can be seen by using the spherical symmetry [4] of the collision operator $\tilde{L}^{\beta\alpha}$. Therefore, using the notations

$$\Psi^\alpha(x_1, \zeta_1, \zeta_\rho) = \Phi^\alpha(x_1, \zeta_1, \zeta_\rho)E^\alpha, \tag{17a}$$

$$\tilde{\mathcal{L}}^{\beta\alpha}(\Psi^\beta, \Psi^\alpha) = (\zeta_\rho/\zeta_2)\tilde{L}^{\beta\alpha}\left(\frac{\zeta_2}{\zeta_\rho}\Phi^\beta, \frac{\zeta_2}{\zeta_\rho}\Phi^\alpha\right)E^\alpha, \tag{17b}$$

we can transform the boundary-value problem (12)–(14) for $\phi_K^\alpha$ into that for $\Psi^\alpha$:

$$\zeta_1\frac{\partial\Psi^\alpha}{\partial x_1} = \sum_{\beta=A,B} K^{\beta\alpha}\tilde{\mathcal{L}}^{\beta\alpha}(X_0^\alpha\Psi^\beta, X_0^\beta\Psi^\alpha), \tag{18}$$

$$\Psi^\alpha = X_0^\alpha\zeta_\rho(-2\hat{m}^\alpha b_I + A^\alpha)E^\alpha, \quad \zeta_1 > 0, \quad x_1 = 0 \quad \text{(problem I)}, \tag{19a}$$

$$\Psi^\alpha = X_0^\alpha\zeta_\rho(-2\hat{m}^\alpha b_{II} + D^{(A)\alpha} - D^{(B)\alpha})E^\alpha, \quad \zeta_1 > 0, \quad x_1 = 0 \quad \text{(problem II)}, \tag{19b}$$

$$\Psi^\alpha \to 0, \quad \text{as} \quad x_1 \to \infty. \tag{20}$$

Note that $E^\alpha$, $A^\alpha$, and $D^{(\beta)\alpha}$ are now the functions of $\zeta_1$ and $\zeta_\rho$ because $\zeta = |\boldsymbol{\zeta}| = (\zeta_1^2 + \zeta_\rho^2)^{1/2}$. Following the transformation by Grad [50] for a single-component gas, one can derive the expression of $\tilde{\mathcal{L}}^{\beta\alpha}$ in terms of integral kernels. That is,

$$\tilde{\mathcal{L}}^{\beta\alpha}(f, g) = \tilde{\mathcal{L}}_1^{\beta\alpha}(f) + \tilde{\mathcal{L}}_2^{\beta\alpha}(g) - \tilde{\mathcal{L}}_3^{\beta\alpha}(f) - \nu^\beta(\zeta)g, \tag{21}$$

with

$$\tilde{\mathcal{L}}_J^{\beta\alpha}(f) = E^\alpha\int_0^\infty d\xi_\rho\int_{-\infty}^\infty d\xi_1\mathcal{K}_J^{\beta\alpha}(\xi_1, \xi_\rho, \zeta_1, \zeta_\rho)f(\xi_1, \xi_\rho) \quad (J = 1, 2, 3), \tag{22}$$

$$\nu^\alpha(\zeta) = \frac{1}{2\sqrt{2}}\left(\frac{1}{\sqrt{\hat{m}^\alpha}}\exp(-\hat{m}^\alpha\zeta^2) + (2\zeta + \frac{1}{\hat{m}^\alpha\zeta})\int_0^{\sqrt{\hat{m}^\alpha}\zeta}\exp(-y^2)dy\right). \tag{23}$$

The explicit form of integral kernels $\mathcal{K}_J^{\beta\alpha}$ $(J = 1, 2, 3)$ is given in the Appendix B.

Substituting Eq. (11) with the similarity solution (16) [and (17a)] into Eqs. (5)–(7), we have the following expression for the macroscopic variables: for problem I,

$$\begin{aligned}
&N^\alpha = -c_I X_0^\alpha x_2, \quad \omega^\alpha = -c_I\hat{m}^\alpha X_0^\alpha x_2, \quad \tau^\alpha = c_I x_2, \quad \chi^\alpha = P^\alpha = 0,\\
&u_i^\alpha = c_I(b_I - \hat{D}_{T\alpha} + U^\alpha)\delta_{i2}, \quad P_{ij}^\alpha = c_I S^\alpha(\delta_{i1}\delta_{j2} + \delta_{i2}\delta_{j1}), \quad Q_i^\alpha = c_I(-\hat{\lambda}^{\alpha\prime}X_0^\alpha + H^\alpha)\delta_{i2},\\
&N = -c_I x_2, \quad \omega = -c_I(\hat{m}^A X_0^A + \hat{m}^B X_0^B)x_2, \quad \tau = c_I x_2, \quad P = 0,\\
&u_i = c_I(b_I + U)\delta_{i2}, \quad P_{ij} = c_I(S^A + S^B)(\delta_{i1}\delta_{j2} + \delta_{i2}\delta_{j1}),\\
&Q_i = c_I\left(-\hat{\lambda}' - \frac{5}{2}(X_0^A\hat{D}_{TA} + X_0^B\hat{D}_{TB}) + H\right)\delta_{i2},
\end{aligned} \tag{24a}$$

and for problem II,

$$\begin{aligned}
&N^\alpha = P^\alpha = \chi^\alpha = c_{II}(\delta_{\alpha A} - \delta_{\alpha B})x_2, \quad \omega^\alpha = c_{II}\hat{m}^\alpha(\delta_{\alpha A} - \delta_{\alpha B})x_2, \quad \tau^\alpha = 0,\\
&u_i^\alpha = c_{II}(b_{II} - \hat{\Delta}_{\alpha A} + \hat{\Delta}_{\alpha B} + U^\alpha)\delta_{i2}, \quad P_{ij}^\alpha = c_{II}[(\delta_{\alpha A} - \delta_{\alpha B})x_2\delta_{ij} + S^\alpha(\delta_{i1}\delta_{j2} + \delta_{i2}\delta_{j1})],\\
&Q_i^\alpha = c_{II}[-X_0^\alpha(\hat{\Gamma}_D^{(A)\alpha} - \hat{\Gamma}_D^{(B)\alpha}) + H^\alpha]\delta_{i2},\\
&N = P = \tau = 0, \quad \omega = c_{II}(\hat{m}^A - \hat{m}^B)x_2, \quad u_i = c_{II}(b_{II} + U)\delta_{i2},\\
&P_{ij} = c_{II}(S^A + S^B)(\delta_{i1}\delta_{j2} + \delta_{i2}\delta_{j1}),\\
&Q_i = c_{II}\left(-(\hat{D}_{TA} - \hat{D}_{TB}) - \frac{5}{2}\sum_{\beta=A,B}X_0^\beta(\hat{\Delta}_{\beta A} - \hat{\Delta}_{\beta B}) + H\right)\delta_{i2},
\end{aligned} \tag{24b}$$

where

$$U^\alpha(x_1) = \frac{\pi}{X_0^\alpha}\int_0^\infty\int_{-\infty}^\infty \zeta_\rho^2 \Psi^\alpha d\zeta_1 d\zeta_\rho, \tag{25a}$$

$$U(x_1) = \Big(\sum_{\beta=A,B} \hat{m}^\beta X_0^\beta U^\beta\Big)/\Big(\sum_{\beta=A,B} \hat{m}^\beta X_0^\beta\Big), \tag{25b}$$

$$S^\alpha(x_1) = 2\pi\hat{m}^\alpha \int_0^\infty\int_{-\infty}^\infty \zeta_1\zeta_\rho^2 \Psi^\alpha d\zeta_1 d\zeta_\rho, \tag{25c}$$

$$H^\alpha(x_1) = \pi\int_0^\infty\int_{-\infty}^\infty \zeta_\rho^2\left(\hat{m}^\alpha(\zeta_1^2+\zeta_\rho^2) - \frac{5}{2}\right)\Psi^\alpha d\zeta_1 d\zeta_\rho, \tag{25d}$$

$$H(x_1) = \sum_{\beta=A,B}\left(H^\beta + \frac{5}{2}X_0^\beta(U^\beta - U)\right). \tag{25e}$$

The functions $U^\alpha$, $U$, $S^\alpha$, $H^\alpha$, and $H$, which we call the Knudsen-layer functions, decay exponentially as $x_1 \to \infty$. In Eqs. (24a) and (24b), they appear only in the $x_2$-component of flow velocities $u_2^\alpha$ and $u_2$, in that of heat-flow vectors $Q_2^\alpha$ and $Q_2$, and in the $x_1x_2$-component of stress tensors $P_{12}^\alpha$ (or $P_{21}^\alpha$) and $P_{12}$ (or $P_{21}$). On the other hand, from the relation (15) we find

$$S^A + S^B = 0, \tag{26}$$

so that the Knudsen-layer function does not appear in the stress tensor $P_{ij}$ of the mixture. The property (26) is used as a measure of accuracy of the numerical solution later. In summary, except $u_2^\alpha$, $u_2$, $Q_2^\alpha$, $Q_2$, and $P_{12}^\alpha$ (or $P_{21}^\alpha$), the macroscopic variables are expressed only by the fluid-dynamic solution: Eq. (10a) multiplied by $c_I$ or Eq. (10b) by $c_{II}$.

As is mentioned in Sec. 3.2, $b_I c_I$ and $b_{II}c_{II}$ are the flow velocity of the mixture away from the wall. On the other hand, the expression of $u_i$ in Eqs. (24a) and (24b) shows that, if the Knudsen-layer function is neglected, the flow velocity of the mixture on the wall ($x_1 = 0$) is also given by

$$\begin{aligned} u_2 &= b_I c_I = b_I\left(\frac{d\tau}{dx_2}\right), \quad \text{for problem I,} \\ u_2 &= b_{II}c_{II} = b_{II}\left(\frac{d\chi^A}{dx_2}\right), \quad \text{for problem II.} \end{aligned} \tag{27}$$

This means that the flow velocity of the fluid-dynamic solution is subject to the slip on the wall caused by the temperature or concentration gradient. From this point of view, the constant $b_I$ is called the coefficient of thermal slip and $b_{II}$ the coefficient of diffusion slip.

# 4 Numerical Analysis

## 4.1 Plan of computation

As is mentioned in the first paragraph in Sec. 3.2, the reduced boundary-value problem (18)–(20) has a solution if and only if the undetermined constant $b$ takes a special value, where $b = b_I$ for problem I and $b = b_{II}$ for problem II. A straightforward way to solve the problem is to repeat computation with different $b$ until a solution satisfying the condition (20) is obtained. However, since such a method is generally inefficient, we adopt the method devised in Ref. [16].

Consider the function

$$\tilde{\Psi}^\alpha(x_1,\zeta_1,\zeta_\rho) = \Psi^\alpha(x_1,\zeta_1,\zeta_\rho) + 2\hat{m}^\alpha X_0^\alpha\,\delta\,\zeta_\rho\,E^\alpha, \tag{28}$$

where $\delta$ is an undetermined constant. Since the second term on the right is a solution of Eq. (18), $\tilde{\Psi}^\alpha$ also satisfies Eq. (18):

$$\zeta_1\frac{\partial\tilde{\Psi}^\alpha}{\partial x_1} = \sum_{\beta=A,B} K^{\beta\alpha}\tilde{\mathcal{L}}^{\beta\alpha}(X_0^\alpha\tilde{\Psi}^\beta, X_0^\beta\tilde{\Psi}^\alpha). \tag{29}$$

The boundary condition for $\tilde{\Psi}^\alpha$ on the wall is obtained from Eqs. (19a) and (19b) with (28) as

$$\tilde{\Psi}^\alpha = X_0^\alpha \zeta_\rho(-2\hat{m}^\alpha b_{I*} + A^\alpha)E^\alpha, \quad \zeta_1 > 0, \quad x_1 = 0, \quad \text{for problem I,} \tag{30a}$$

$$\tilde{\Psi}^\alpha = X_0^\alpha \zeta_\rho(-2\hat{m}^\alpha b_{II*} + D^{(A)\alpha} - D^{(B)\alpha})E^\alpha, \quad \zeta_1 > 0, \quad x_1 = 0, \quad \text{for problem II,} \tag{30b}$$

where

$$b_{I*} = b_I - \delta, \quad b_{II*} = b_{II} - \delta. \tag{31}$$

Since $\Psi^\alpha$ decays exponentially (see the first paragraph in Sec. 3.2), it is negligible at a distance large enough, say at $x_1 = d$. Consequently $\tilde{\Psi}^\alpha$ at $x_1 = d$ can be written as

$$\tilde{\Psi}^\alpha(d, \zeta_1, \zeta_\rho) = 2\hat{m}^\alpha X_0^\alpha \, \delta \, \zeta_\rho E^\alpha. \tag{32}$$

The corresponding flow velocity $\tilde{U}(x_1)$ of the mixture, which is defined by Eq. (25b) [with (25a)] with $\Psi^\alpha$ replaced by $\tilde{\Psi}^\alpha$, takes the value $\delta$:

$$\tilde{U}(d) = \delta. \tag{33}$$

Because of Eq. (32), $\tilde{\Psi}^\alpha$ satisfies the reflection condition at $x_1 = d$:

$$\tilde{\Psi}^\alpha(d, \zeta_1, \zeta_\rho) = \tilde{\Psi}^\alpha(d, -\zeta_1, \zeta_\rho). \tag{34}$$

We solve the boundary-value problem (29), (30a) [or (30b)], and (34) for a given $b_{I*}$ (or $b_{II*}$), instead of solving the original problem (18)–(20) directly. Once $\tilde{\Psi}^\alpha$ is obtained, $\delta$ is determined by Eq. (33). Then, $\Psi^\alpha$ and $b_I$ (or $b_{II}$) are obtained from Eqs. (28) and (31).

## 4.2 Finite-difference scheme

Because of the factor $E^\alpha$ [see Eqs. (16) and (28)], $\tilde{\Psi}^\alpha$ is expected to decay rapidly as $|\zeta_1|$ or $\zeta_\rho$ tends to $\infty$. Thus in the actual computation we restrict the regions of $\zeta_1$ and $\zeta_\rho$ to finite ones. That is, for a proper choice of $Z_1^\alpha (> 0)$ and $Z_\rho^\alpha (> 0)$, we carry out the numerical computation for $\tilde{\Psi}^\alpha$ in the region $0 \le x_1 \le d$, $-Z_1^\alpha \le \zeta_1 \le Z_1^\alpha$, and $0 \le \zeta_\rho \le Z_\rho^\alpha$. The regions of $x_1$, $\zeta_1$, and $\zeta_\rho$ are divided into $N_x$, $4N_1$, and $2N_\rho$ intervals in the following way:

$$\begin{aligned}
&0 = x_1^{(0)} < x_1^{(1)} < \cdots < x_1^{(N_x)} = d, \\
&-Z_1^\alpha = \zeta_1^{\alpha(-2N_1)} < \zeta_1^{\alpha(-2N_1+1)} < \cdots < \zeta_1^{\alpha(0)} (= 0) < \zeta_1^{\alpha(1)} < \cdots < \zeta_1^{\alpha(2N_1)} = Z_1^\alpha, \\
&0 = \zeta_\rho^{\alpha(0)} < \zeta_\rho^{\alpha(1)} < \cdots < \zeta_\rho^{\alpha(2N_\rho)} = Z_\rho^\alpha.
\end{aligned}$$

Here, $Z_1^\alpha$ and $Z_\rho^\alpha$ are taken to be $Z_1^\alpha = Z_1/\sqrt{\hat{m}^\alpha}$ and $Z_\rho^\alpha = Z_\rho/\sqrt{\hat{m}^\alpha}$ with $Z_1$ and $Z_\rho$ being constants common to $\tilde{\Psi}^A$ and $\tilde{\Psi}^B$. For the later convenience, chiefly for the computation of collision integrals, the lattice points of $\zeta_1$ are chosen to be symmetric with respect to $\zeta_1 = 0$, i.e., $\zeta_1^{\alpha(j)} = -\zeta_1^{\alpha(-j)}$. We denote the value of a physical quantity at a lattice point by attaching the subscript label corresponding to the point, e.g., $\tilde{\Psi}^\alpha_{(i,j,k)} = \tilde{\Psi}^\alpha(x_1^{(i)}, \zeta_1^{\alpha(j)}, \zeta_\rho^{\alpha(k)})$. For steady and spatially one-dimensional problems, it is known that the velocity distribution function is, in general, discontinuous at $\zeta_1 = 0$ on the wall ($x_1 = 0$) (see, for instance, Ref. [51]). Thus $\tilde{\Psi}^\alpha$ has two limiting values $\tilde{\Psi}^\alpha(0, \pm 0, \zeta_\rho)$ on the wall. Taking it into account, we prepare two sets of values $\tilde{\Psi}^\alpha_{(0,\pm 0,k)}$ for the lattice point $(0, 0, \zeta_\rho^{\alpha(k)})$ in the computation.

We obtain the discrete solution $\tilde{\Psi}^\alpha_{(i,j,k)}$ as the limit of the sequence $\{\tilde{\Psi}^{\alpha(n)}_{(i,j,k)}\}$ $(n = 0, 1, 2, \dots)$ constructed by the iteration using the following finite-difference scheme for Eq. (29):

$$\zeta_1^{\alpha(j)} \nabla_{ijk} \tilde{\Psi}^{\alpha(n+1)} = -\tilde{\nu}^\alpha_{(j,k)} \tilde{\Psi}^{\alpha(n+1)}_{(i,j,k)} + C^{\alpha(n)}_{(i,j,k)}, \tag{35}$$

where $\nabla_{ijk}$ corresponds to $\partial/\partial x_1$, and $\tilde{\nu}^{\alpha}_{(j,k)}$ and $C^{\alpha(n)}_{(i,j,k)}$ are defined as

$$\tilde{\nu}^{\alpha}_{(j,k)} = K^{A\alpha} X_0^A \nu^A(\zeta_1^{\alpha(j)}, \zeta_\rho^{\alpha(k)}) + K^{B\alpha} X_0^B \nu^B(\zeta_1^{\alpha(j)}, \zeta_\rho^{\alpha(k)}), \tag{36a}$$

$$C^{A(n)}_{(i,j,k)} = [K^{AA} X_0^A (\tilde{\mathcal{L}}_1^{AA} + \tilde{\mathcal{L}}_2^{AA} - \tilde{\mathcal{L}}_3^{AA}) + K^{BA} X_0^B \tilde{\mathcal{L}}_2^{BA}](\tilde{\Psi}^{A(n)})_{(i,j,k)} + K^{BA} X_0^A (\tilde{\mathcal{L}}_1^{BA} - \tilde{\mathcal{L}}_3^{BA})(\tilde{\Psi}^{B(n)})_{(i,j,k)}, \tag{36b}$$

$$C^{B(n)}_{(i,j,k)} = [K^{BB} X_0^B (\tilde{\mathcal{L}}_1^{BB} + \tilde{\mathcal{L}}_2^{BB} - \tilde{\mathcal{L}}_3^{BB}) + K^{AB} X_0^A \tilde{\mathcal{L}}_2^{AB}](\tilde{\Psi}^{B(n)})_{(i,j,k)} + K^{AB} X_0^B (\tilde{\mathcal{L}}_1^{AB} - \tilde{\mathcal{L}}_3^{AB})(\tilde{\Psi}^{A(n)})_{(i,j,k)}. \tag{36c}$$

For $\nabla_{ijk}$, the following formulas are used: for $1 \le j \le 2N_1$,

$$\nabla_{ijk}\tilde{\Psi}^{\alpha(n)} = \begin{cases} (\tilde{\Psi}^{\alpha(n)}_{(1,j,k)} - \tilde{\Psi}^{\alpha(n)}_{(0,j,k)})/h_1 & (i=1), \\ w_0(h_{i-1},h_i)\tilde{\Psi}^{\alpha(n)}_{(i,j,k)} - w_1(h_{i-1},h_i)\tilde{\Psi}^{\alpha(n)}_{(i-1,j,k)} + w_2(h_{i-1},h_i)\tilde{\Psi}^{\alpha(n)}_{(i-2,j,k)} & (2 \le i \le N_x), \end{cases} \tag{37a}$$

and for $-2N_1 \le j \le 0$,

$$\nabla_{ijk}\tilde{\Psi}^{\alpha(n)} = \begin{cases} (2\tilde{\Psi}^{\alpha(n)}_{(N_x,j,k)} - \frac{3}{2}\tilde{\Psi}^{\alpha(n)}_{(N_x-1,j,k)} - \frac{1}{2}\tilde{\Psi}^{\alpha(n)}_{(N_x-1,-j,k)})/h_{N_x} & (i = N_x - 1), \\ -w_2(h_{i+2},h_{i+1})\tilde{\Psi}^{\alpha(n)}_{(i+2,j,k)} + w_1(h_{i+2},h_{i+1})\tilde{\Psi}^{\alpha(n)}_{(i+1,j,k)} - w_0(h_{i+2},h_{i+1})\tilde{\Psi}^{\alpha(n)}_{(i,j,k)} & (0 \le i \le N_x - 2), \end{cases} \tag{37b}$$

where

$$h_i = x_1^{(i)} - x_1^{(i-1)}, \quad w_0(a,b) = \frac{a+2b}{b(a+b)}, \quad w_1(a,b) = \frac{a+b}{ab}, \quad w_2(a,b) = \frac{b}{a(a+b)}. \tag{38}$$

The terms $C^{\alpha(n)}_{(i,j,k)}$ are computed by the numerical kernel method first proposed in Ref. [27] for a single-component gas. The details of the method is given in Sec. 4.3. The functions $A^\alpha$ and $D^{(\beta)\alpha}$, which are the solutions of Eqs. (9a) and (9b), appear in the boundary conditions (30a) and (30b). In the present work, we use their accurate numerical data obtained in Ref. [42] for arbitrary values of $X_0^A$ for a binary mixture of hard-sphere gases.

The solution procedure is as follows. Start with appropriate initial data $\tilde{\Psi}^{\alpha(0)}_{(i,j,k)}$ and $b_*$. Suppose that $\tilde{\Psi}^{\alpha(n)}_{(i,j,k)}$ is known. Then $\tilde{\Psi}^{\alpha(n+1)}_{(i,j,k)}$ is computed by the following process.

(i) Compute $C^{\alpha(n)}_{(i,j,k)}$ using $\tilde{\Psi}^{A(n)}_{(i,j,k)}$ and $\tilde{\Psi}^{B(n)}_{(i,j,k)}$.

(ii) Using the boundary condition (30a) [or (30b)], compute $\tilde{\Psi}^{\alpha(n+1)}_{(i,j,k)}$ $(1 \le j \le 2N_1)$ from $i = 1$ to $N_x$ successively by Eq. (35) with (37a).

(iii) Compute $\tilde{\Psi}^{\alpha(n+1)}_{(N_x,j,k)}$ $(-1 \ge j \ge -2N_1)$ using the boundary condition (34). Since the lattice points of $\zeta_1$ is symmetric with respect to $\zeta_1 = 0$, $\tilde{\Psi}^{\alpha(n+1)}_{(N_x,j,k)}$ is given by $\tilde{\Psi}^{\alpha(n+1)}_{(N_x,j,k)} = \tilde{\Psi}^{\alpha(n+1)}_{(N_x,-j,k)}$.

(iv) Compute $\tilde{\Psi}^{\alpha(n+1)}_{(i,j,k)}$ $(-1 \ge j \ge -2N_1)$ from $i = N_x - 1$ to 0 successively by Eq. (35) with (37b), using the data $\tilde{\Psi}^{\alpha(n+1)}_{(N_x,j,k)}$ obtained in (iii).

(v) Compute $\tilde{\Psi}^{\alpha(n+1)}_{(0,-0,k)}$ and $\tilde{\Psi}^{\alpha(n+1)}_{(i,0,k)}$ $(i = 1, \ldots, N_x)$ by Eq. (35) with $\zeta_1^{(j)} = 0$. Compute $\tilde{\Psi}^{\alpha(n+1)}_{(0,+0,k)}$ by the boundary condition (30a) [or (30b)].

We repeat steps (i)–(v) for $n = 0, 1, 2, \ldots$ until $\tilde{\Psi}^{\alpha(n)}_{(i,j,k)}$ converges. Then $\Psi^{\alpha}_{(i,j,k)}$ and $b$ are obtained by Eqs. (28) and (31) with Eq. (33). The Knudsen-layer functions are obtained from the (discrete) solution by the integrations [Eqs. (25a)–(25d)] using Simpson's formula.

In the actual computation, we repeat the above process with new $b$ as $b_*$ in order to reduce the errors coming from the second term on the right-hand side of Eq. (28).

## 4.3 Numerical kernel method

In order to obtain $C^{\alpha(n)}_{(i,j,k)}$, we have to carry out the complicated five-fold integrations numerically, which requires heavy computation. In Ref. [27], an accurate and efficient method for the computation of collision integrals was proposed for a single-component gas. We apply this method to the computation of $C^{\alpha(n)}_{(i,j,k)}$. We first introduce the following piecewise quadratic functions $B^{\alpha\pm}_{l,m}(\zeta_1,\zeta_\rho)$ of $\zeta_1$ and $\zeta_\rho$, localized around the lattice point $(\zeta_1^{\alpha(l)},\zeta_\rho^{\alpha(m)})$:

$$B^{\alpha\pm}_{l,m}(\zeta_1,\zeta_\rho)=Y_l^{\alpha\zeta_1}(\zeta_1)\chi_{[0,Z_1^\alpha]}(\pm\zeta_1)Y_m^{\alpha\zeta_\rho}(\zeta_\rho)\chi_{[0,Z_\rho^\alpha]}(\zeta_\rho), \tag{39}$$

where $Y_l^{\alpha z}(y)$ with $y=\zeta_1,\zeta_\rho$ and $z=\zeta_1,\zeta_\rho$ are defined by

$$Y^{\alpha z}_{2m}(y)=\begin{cases}\dfrac{(y-z^{\alpha(2m+2)})(y-z^{\alpha(2m+1)})}{(z^{\alpha(2m)}-z^{\alpha(2m+2)})(z^{\alpha(2m)}-z^{\alpha(2m+1)})}, & \text{for } z^{\alpha(2m)}<y<z^{\alpha(2m+2)},\\ \dfrac{(y-z^{\alpha(2m-2)})(y-z^{\alpha(2m-1)})}{(z^{\alpha(2m)}-z^{\alpha(2m-2)})(z^{\alpha(2m)}-z^{\alpha(2m-1)})}, & \text{for } z^{\alpha(2m-2)}<y<z^{\alpha(2m)},\\ 0, \quad \text{otherwise,}\end{cases} \tag{40a}$$

$$Y^{\alpha z}_{2m+1}(y)=\begin{cases}\dfrac{(y-z^{\alpha(2m+2)})(y-z^{\alpha(2m)})}{(z^{\alpha(2m+1)}-z^{\alpha(2m+2)})(z^{\alpha(2m+1)}-z^{\alpha(2m)})}, & \text{for } z^{\alpha(2m)}<y<z^{\alpha(2m+2)},\\ 0, \quad \text{otherwise.}\end{cases} \tag{40b}$$

In Eq. (39), $\chi_{[a,b]}(y)$ denotes the characteristic function of the interval $[a,b]$, i.e., $\chi_{[a,b]}(y)=1$ for $a\le y\le b$ and $\chi_{[a,b]}(y)=0$ otherwise. Then we expand $\tilde\Psi^{\alpha(n)}$ at $x_1=x_1^{(i)}$ in terms of $B^{\alpha\pm}_{l,m}(\zeta_1,\zeta_\rho)$ as follows:

$$\tilde\Psi^{\alpha(n)}(x_1^{(i)},\zeta_1,\zeta_\rho)=\sum_{m=0}^{2N_\rho}\sum_{l=0}^{2N_1}\left(\tilde\Psi^{\alpha(n)}_{(i,l,m)}B^{\alpha+}_{l,m}(\zeta_1,\zeta_\rho)+\tilde\Psi^{\alpha(n)}_{(i,-l,m)}B^{\alpha-}_{-l,m}(\zeta_1,\zeta_\rho)\right). \tag{41}$$

In the above expression and in Eqs. (42a) and (42b) below, the $\tilde\Psi^{\alpha(n)}_{(i,l,m)}$ and $\tilde\Psi^{\alpha(n)}_{(i,-l,m)}$ for $i=l=0$ should be regarded as $\tilde\Psi^{\alpha(n)}_{(0,+0,m)}$ and $\tilde\Psi^{\alpha(n)}_{(0,-0,m)}$ because $\tilde\Psi^{\alpha}$ is discontinuous at $\zeta_1=0$ on the wall. Substitution of Eq. (41) into Eqs. (36b) and (36c) gives the following expression for $C^{\alpha(n)}_{(i,j,k)}$:

$$C^{A(n)}_{(i,j,k)}=\sum_{m=0}^{2N_\rho}\sum_{l=0}^{2N_1}\left(C^{AA+}_{j,k,l,m}\tilde\Psi^{A(n)}_{(i,l,m)}+C^{BA+}_{j,k,l,m}\tilde\Psi^{B(n)}_{(i,l,m)}+C^{AA-}_{j,k,-l,m}\tilde\Psi^{A(n)}_{(i,-l,m)}+C^{BA-}_{j,k,-l,m}\tilde\Psi^{B(n)}_{(i,-l,m)}\right), \tag{42a}$$

$$C^{B(n)}_{(i,j,k)}=\sum_{m=0}^{2N_\rho}\sum_{l=0}^{2N_1}\left(C^{AB+}_{j,k,l,m}\tilde\Psi^{A(n)}_{(i,l,m)}+C^{BB+}_{j,k,l,m}\tilde\Psi^{B(n)}_{(i,l,m)}+C^{AB-}_{j,k,-l,m}\tilde\Psi^{A(n)}_{(i,-l,m)}+C^{BB-}_{j,k,-l,m}\tilde\Psi^{B(n)}_{(i,-l,m)}\right), \tag{42b}$$

where

$$C^{AA\pm}_{j,k,l,m}=[K^{AA}X_0^A(\tilde{\mathcal{L}}_1^{AA}+\tilde{\mathcal{L}}_2^{AA}-\tilde{\mathcal{L}}_3^{AA})+K^{BA}X_0^B\tilde{\mathcal{L}}_2^{BA}](B^{A\pm}_{l,m})_{(j,k)}, \tag{43a}$$

$$C^{BA\pm}_{j,k,l,m}=K^{BA}X_0^A(\tilde{\mathcal{L}}_1^{BA}-\tilde{\mathcal{L}}_3^{BA})(B^{B\pm}_{l,m})_{(j,k)}, \tag{43b}$$

$$C^{AB\pm}_{j,k,l,m}=K^{AB}X_0^B(\tilde{\mathcal{L}}_1^{AB}-\tilde{\mathcal{L}}_3^{AB})(B^{A\pm}_{l,m})_{(j,k)}, \tag{43c}$$

$$C^{BB\pm}_{j,k,l,m}=[K^{BB}X_0^B(\tilde{\mathcal{L}}_1^{BB}+\tilde{\mathcal{L}}_2^{BB}-\tilde{\mathcal{L}}_3^{BB})+K^{AB}X_0^A\tilde{\mathcal{L}}_2^{AB}](B^{B\pm}_{l,m})_{(j,k)}. \tag{43d}$$

We call $C^{A\alpha\pm}_{j,k,l,m}$ and $C^{B\alpha\pm}_{j,k,l,m}$ the numerical kernels of $C^{\alpha(n)}_{(i,j,k)}$. Note that $C^{\beta\alpha\pm}_{j,k,l,m}$ $(\alpha,\beta=A,B)$ is the integral of a given function and can be computed beforehand. The $C^{\beta\alpha\pm}_{j,k,l,m}$ has the property

$$C^{\beta\alpha-}_{j,k,-l,m}=C^{\beta\alpha+}_{-j,k,l,m}, \tag{44}$$

because of the symmetry property of $\tilde{\mathcal{L}}_J^{\beta\alpha}$ $(J = 1, 2, 3)$ and the lattice of $\zeta_1$ symmetric with respect to $\zeta_1 = 0$. Further, $K^{\beta\alpha}$ and $X_0^A$ are not contained in the integrals $\tilde{\mathcal{L}}_1^{AA}(B_{l,m}^{A+})$, $\tilde{\mathcal{L}}_2^{BA}(B_{l,m}^{A+})$, etc. Thus we prepare the database of $\tilde{\mathcal{L}}_1^{\beta\alpha}(B_{l,m}^{\beta+})_{(j,k)}$, $\tilde{\mathcal{L}}_2^{\beta\alpha}(B_{l,m}^{\alpha+})_{(j,k)}$, and $\tilde{\mathcal{L}}_3^{\beta\alpha}(B_{l,m}^{\beta+})_{(j,k)}$ for different values of $\hat{m}^B$ for $j = -2N_1, \ldots, 2N_1$, $l = 0, \ldots, 2N_1$, and $k, m = 0, \ldots, 2N_\rho$. The integration is performed accurately numerically by the Gauss-Legendre formula [52]. Then the numerical kernel $C_{j,k,l,m}^{\beta\alpha\pm}$ is constructed from the database before the process of iteration by Eqs. (43a)–(43d). In the process of iteration, the computation of the collision integrals is a simple multiplication of matrices, i.e., Eqs. (42a) and (42b), and thus is performed efficiently.

### 4.4 Chebyshev polynomials

One of the purposes of the present work is to provide the data for the slip boundary condition for the fluid-dynamic type system derived in Ref. [5] (See Sec. 1). The slip condition is a linear combination of the thermal-slip and the diffusion-slip conditions given in Eq. (27). As is seen from Sec. 3.2, the slip coefficients $b_I$ and $b_{II}$ in Eq. (27) depend on the concentration $X_0^A$. But in the physical situations investigated in Ref. [5] the concentration generally varies along the boundary. Accordingly it is required to prepare formulas from which the values of $b_I$ and $b_{II}$ are readily obtained for arbitrary values of $X_0^A$. We use the Chebyshev polynomial approximation [53] with respect to $X_0^A$ to meet this requirement. This approximation is useful not only for the slip coefficients but also for other physical quantities such as the Knudsen-layer functions. Therefore we describe it in general form.

Let us denote by $T_n$ $(n = 0, 1, 2, \ldots)$ the Chebyshev polynomial defined for $0 \leq \theta \leq \pi$ by the relation

$$T_n(\cos\theta) = \cos n\theta. \tag{45}$$

Any function $F$ of $X_0^A$ can be approximated by the polynomials of degree up to $N$ in the Chebyshev basis as

$$F(X_0^A) = \sum_{n=0}^{N} a_n T_n(2X_0^A - 1), \tag{46}$$

where

$$a_n = \frac{1}{N\epsilon_n} \sum_{k=0}^{N-1} [F_k T_n(y_k) + F_{k+1} T_n(y_{k+1})], \tag{47}$$

with $\epsilon_0 = \epsilon_N = 2$ and $\epsilon_1 = \cdots = \epsilon_{N-1} = 1$, and

$$F_k = F(\frac{1 + y_k}{2}), \tag{48}$$

with $y_k$ being the Chebyshev abscissa:

$$y_k = \cos(k\frac{\pi}{N}) \quad (k = 0, 1, \ldots, N). \tag{49}$$

The approximation (46) takes the exact value of $F$ at $X_0^A = (1 + y_k)/2$.

Since the function $F$ of $X_0^A$ is arbitrary, any physical quantity for an arbitrary value of $X_0^A$ can be obtained by the formula (46) from its data computed at $N + 1$ discrete values of $X_0^A$, i.e., $X_0^A = (1 + y_k)/2$ $(k = 0, 1, \ldots, N)$.

## 5 Results and Discussions

In the present paper, we carry out the computation for $m^B/m^A = 2, 4, 5$, and 10 and for various values of $X_0^A$, restricting ourselves to the case $d^B/d^A = 1$. The computation for other values of $d^B/d^A$ can be performed by using the same code and database of $\tilde{\mathcal{L}}_1^{\beta\alpha}(B_{l,m}^{\beta+})_{(j,k)}$, $\tilde{\mathcal{L}}_2^{\beta\alpha}(B_{l,m}^{\alpha+})_{(j,k)}$, etc. In what follows, we assume that $m^B/m^A \geq 1$, because the results for $m^B/m^A < 1$ can be obtained from those for $m^B/m^A > 1$ by a simple transformation.

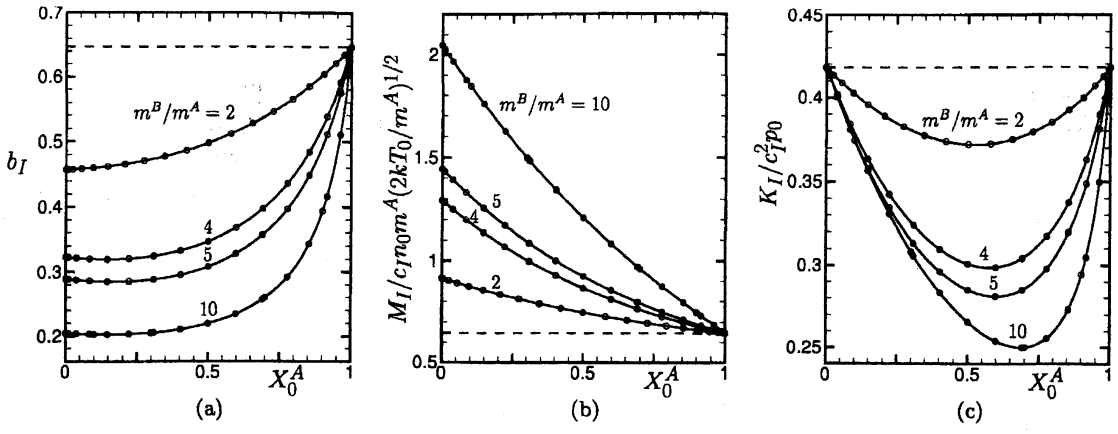


Figure 1: Coefficient of thermal slip $b_I$ and related quantities. (a) Slip coefficient $b_I$, (b) momentum $M_I$ away from the wall, and (c) kinetic energy $K_I$ per unit volume away from the wall. Both closed and open circles indicate the present result. The solid line indicates the present result using the formula (51). The data used to construct the formula are marked with closed circle. The dashed line indicates the result for $m^B/m^A = 1$.

In the present computation, the velocity space is commonly limited to $-4.5 \le \sqrt{\hat{m}^\alpha}\zeta_1^\alpha \le 4.5$ and $0 \le \sqrt{\hat{m}^\alpha}\zeta_\rho^\alpha \le 4.5$ (i.e., $Z_1 = Z_\rho = 4.5$; see the first paragraph of Sec. 4.2), and there are $101 \times 55$ (problem I) or $101 \times 49$ (problem II) grid points in the domain of $(\zeta_1^\alpha, \zeta_\rho^\alpha)$. The $x_1$-space is limited to $0 \le x_1 \le 24.08$ (i.e., $d = 24.08$) for problem I and for problem II in the case of $m^B/m^A = 2$ and to $0 \le x_1 \le 32.20$ (i.e., $d = 32.20$) for problem II in the case of $m^B/m^A = 4$, 5, and, 10 (see Sec. 4.1). There are 301 grid points for the former and 341 points for the latter.

## 5.1 Slip coefficient

The coefficient of thermal slip $b_I$ vs the concentration $X_0^A$ of gas A is shown in Fig. 1(a). Since $b_I$ is positive, the flow induced along the wall is in the direction from the colder part to the hotter at a large distance from the wall. The $b_I$ is larger for smaller molecular mass ratio $m^B/m^A$ and becomes largest at $m^B/m^A = 1$. For $m^B/m^A = 1$, it is independent of $X_0^A$ because there is no difference (except "color" or "label") between molecules of different kind. For $m^B/m^A = 2$, $b_I$ increases monotonically with increasing $X_0^A$, the concentration of the gas with smaller molecular mass. In contrast, for $m^B/m^A = 4, 5$, and 10, $b_I$ first decreases slightly, takes the minimum at around $X_0^A = 0.15 \sim 0.25$, and then increases monotonically as $X_0^A$ increases from zero to 1. At $X_0^A = 1$, $b_I$ is independent of $m^B/m^A$ because of the absence of gas B. Incidentally, the values at $X_0^A = 0$, where gas A is absent, are equal to the value at $X_0^A = 1$ multiplied by $(m^B/m^A)^{-1/2}$. This relation is easily seen by changing the reference molecular mass from $m^A$ to $m^B$.

The slip coefficient $b_I$ corresponds to the flow velocity of the mixture away from the wall when $c_I = 1$. The momentum $(0, M_I, 0)$ and the kinetic energy $K_I$ per unit volume of the mixture away from the wall is related to $b_I$ as follows:

$$\begin{aligned} M_I/c_I n_0 m^A (2kT_0/m^A)^{1/2} &= \hat{\rho}_0 b_I, \\ K_I/c_I^2 p_0 &= \hat{\rho}_0 b_I^2, \end{aligned} \tag{50}$$

where $\hat{\rho}_0 (\equiv \hat{m}^A X_0^A + \hat{m}^B X_0^B) = (1 - \hat{m}^B) X_0^A + \hat{m}^B$. These quantities vs $X_0^A$ are shown in Figs. 1(b) and 1(c). The momentum is larger for larger $m^B/m^A$. It decreases monotonically as $X_0^A$ increases. The values at $X_0^A = 0$ are the same as the value at $X_0^A = 1$ multiplied by $(m^B/m^A)^{1/2}$. The kinetic energy is larger for smaller difference of mass. It takes the same value at $X_0^A = 0$ and 1 and attains the minimum at an intermediate value of $X_0^A$ ($X_0^A = 0.5 \sim 0.7$).

The coefficient of diffusion slip $b_{II}$ vs $X_0^A$ is shown in Fig. 2(a). Since $b_{II}$ is positive, the flow induced along the wall in the far field is in the direction of increasing $X_0^A + \tilde{C}_{II}^A X_2$, i.e., from the part with lower concentration of the gas with smaller molecular mass to the part with higher concentration of the same gas. The $b_{II}$ increases monotonically as $X_0^A$ increases. It is larger for larger mass ratio $m^B/m^A$ when $X_0^A \gtrsim 0.5$. For smaller values of $X_0^A$, however, its dependence on $m^B/m^A$ is not monotonic, and

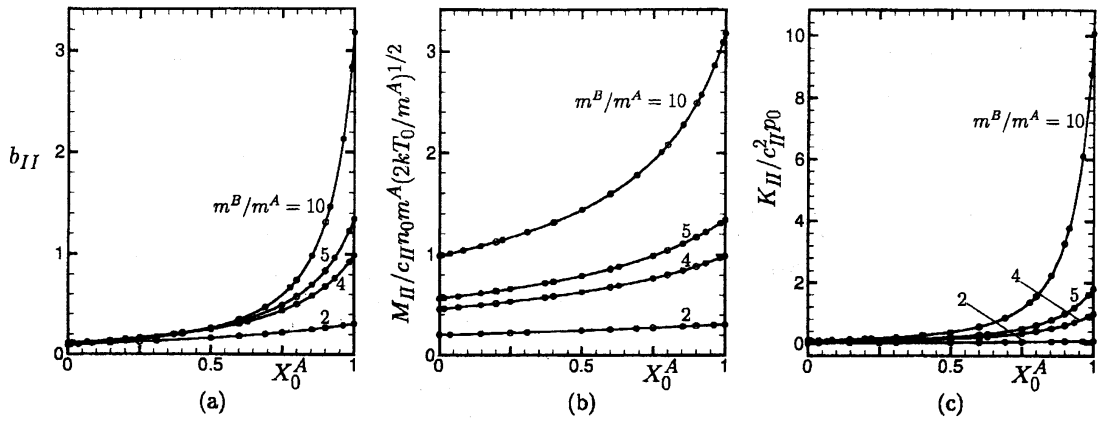


Figure 2: Coefficient of diffusion slip $b_{II}$ and related quantities. (a) Slip coefficient $b_{II}$, (b) momentum $M_{II}$ away from the wall, and (c) kinetic energy $K_{II}$ per unit volume away from the wall. See the caption of Fig. 1.

it becomes largest at around $m^B/m^A = 4$ or 5. For $m^B/m^A = 1$, where there is no difference between molecules of different kind, $b_{II}$ vanishes and thus the diffusion-slip flow is not induced. This fact can be shown analytically by making use of a property of $D^{(\beta)\alpha}$ given in the Appendix B of Ref. [54] and the existence and uniqueness theorem for the Knudsen-layer problem for a single-component gas (see the Appendix C). In the meantime, $b_{II}$ is non-zero at $X_0^A = 0$ and 1. It appears strange at a glance because the "mixture" in these cases is, in reality, a single-component gas, where there is no diffusion-slip flow. However, at $X_0^A = 0$ and 1, the concentration gradient $\tilde{C}_{II}^A$ (or $c_{II}$) should vanish because $0 \leq X_0^A + \tilde{C}_{II}^A X_2 \leq 1$ by definition. Therefore, the diffusion-slip flow, which is the product of $b_{II}$ and $c_{II}$, vanishes, and no contradiction arises.

The induced momentum $(0, M_{II}, 0)$ and the kinetic energy $K_{II}$ per unit volume of the mixture away from the wall are shown in Figs. 2(b) and 2(c). They are related to the slip coefficient $b_{II}$ through Eq. (50) with the subscript $I$ being replaced by the subscript $II$. Both $M_{II}$ and $K_{II}$ are larger for larger $m^B/m^A$ and for larger $X_0^A$.

As is seen from Figs. 1 and 2, the dependence of $\hat{\rho}_0 b_J$ $(J = I, II)$ [cf. the first equation in Eq. (50) and the corresponding relation for $M_{II}$] on $X_0^A$ is simpler than that of $b_J$. Therefore we make the approximation formula of $b_J$ for arbitrary values of $X_0^A$ by applying Eq. (46) to $\hat{\rho}_0 b_J$, not directly to $b_J$ itself. The data used to make the formula are shown with closed circle in Figs. 1 and 2. The resulting formula is

$$b_J = \sum_{n=0}^{N} b_J^{(n)} T_n(2X_0^A - 1)/\hat{\rho}_0 \quad (J = I, II), \tag{51}$$

with $\hat{\rho}_0 = (1 - \hat{m}^B)X_0^A + \hat{m}^B$ and the data of $b_I^{(n)}$ and $b_{II}^{(n)}$ listed in Tables I and II. The solid lines in Figs. 1 and 2 are drawn by using this formula. Some of the values of $b_I$ and $b_{II}$ obtained by Eq. (51) are shown in Table III. The number of the polynomials $N$ in Eq. (51) is taken large enough, so that the data in the table are estimated to be the same as those obtained by direct computation.

The thermal-slip and the diffusion-slip problems have been studied by various approximation methods (the variational method, the moment method, etc.) or by direct computation of the model Boltzmann equation. In contrast, in the present paper, the problems are analyzed faithfully and accurately on the basis of the Boltzmann equation. As a result, the validity of the existing results can be assessed by the present result. A comparison is made in Fig. 3 for this purpose. It is seen that among the existing results the formula proposed by Ivchenko et al. [25] (ILT2, for short) is closest to the present result. It is the improved version of their previous formula [20] (ILT1, for short) based on a special kind of half-space moment method. ILT1 is the same as Loyalka's formula [14] based on the variational method. The results by Yalamov et al. [19] (half-space moment method) and by Sharipov and Kalempa [26] (finite-difference analysis based on the McCormack model [55]) are close to ILT1 rather than to the present result.

Table I: Coefficient $b_I^{(n)}$ $(n = 0, \ldots, N)$ in Eq. (51) for the thermal-slip coefficient $b_I$.

| | $m^B/m^A$ | | | |
|---|---|---|---|---|
| $n$ | 2 (N=5) | 4 (N=8) | 5 (N=8) | 10 (N=16) |
| 0 | 7.63642(−1)* | 9.17923(−1) | 9.84826(−1) | 1.27740 |
| 1 | −1.32632(−1) | −3.17398(−1) | −3.92397(−1) | −6.90326(−1) |
| 2 | 1.66396(−2) | 5.12603(−2) | 6.06550(−2) | 6.84937(−2) |
| 3 | −1.25175(−3) | −5.74465(−3) | −7.00442(−3) | −8.19729(−3) |
| 4 | 1.02588(−4) | 5.45554(−4) | 5.60533(−4) | −3.54147(−4) |
| 5 | −8.94758(−6) | −1.01207(−4) | −1.47912(−4) | −3.84175(−4) |
| 6 | – | 8.14885(−6) | 4.05181(−6) | −8.99259(−5) |
| 7 | – | −1.85388(−6) | −3.97989(−6) | −3.47191(−5) |
| 8 | – | 1.63769(−7) | −1.31647(−7) | −1.14587(−5) |
| 9 | – | – | – | −4.32605(−6) |
| 10 | – | – | – | −1.59296(−6) |
| 11 | – | – | – | −5.67010(−7) |
| 12 | – | – | – | −1.86957(−7) |
| 13 | – | – | – | −8.23480(−8) |
| 14 | – | – | – | −4.14764(−8) |
| 15 | – | – | – | −1.55678(−8) |
| 16 | – | – | – | 8.94466(−10) |

* Read as $7.63642 \times 10^{-1}$.

## 5.2 Knudsen-layer functions and velocity distribution functions

The Knudsen-layer functions of component gases $U^A$ and $U^B$ for the thermal slip (problem I) are shown in Fig. 4. Each function decays monotonically and rapidly to zero as the distance from the wall increases. On one hand, the functions depend monotonically on the mass ratio $m^B/m^A$. The function $U^A$ depends largely for small $X_0^A$, the concentration of the gas with smaller molecular mass, while $U^B$ is little influenced by the value of $X_0^A$. On the other hand, $U^A$ depend on $X_0^A$ especially when $m^B/m^A$ is large. This is also true for $U^B$, but less dependent on $X_0^A$.

The Knudsen-layer functions $U^A$ and $U^B$ for the diffusion slip (problem II) are shown in Fig. 5. They decay rapidly as $x_1 \to \infty$, but the way of decay is non-monotonic for $U^B$. It is clearly seen that the magnitude of $U^A$ decreases with increasing $X_0^A$ while that of $U^B$ increases.

Incidentally, some of the results for $X_0^A = 0.25$, 0.75, and 0.9 in the figures in this section are obtained by applying the formula (46) to the functions $U^A$ and $U^B$ for problem I and to $X_0^A U^A$ and $X_0^B U^B$ for problem II. The FORTRAN code generating the Knudsen-layer functions, not only $U^A$ and $U^B$ but also $H^A$, $H^B$ etc., for an arbitrary value of $X_0^A$ is available from the authors.

Figures 6 and 7 show the reduced velocity distribution functions $\Psi^A$ and $\Psi^B$ and their contour plots for the thermal-slip problem (problem I) in the case of $m^B/m^A = 5$ and $X_0^A = 0.5$. There is a discontinuity at $\zeta_1 = 0$ on the wall ($x_1 = 0$) [see Figs. 6(a) and 7(a)]. The discontinuity disappears inside the gas. This is because the characteristic line of the Boltzmann equation (18) along $\zeta_1 = 0$ does not enter the gas region, so that the discontinuity does not propagate into the gas. [51] Its trace remains, however, as a steep gradient around $\zeta_1 = 0$ near the wall [see Figs. 6(b) and 7(b)]. As the distance from the wall increases, $\Psi^\alpha$ is deformed chiefly around $\zeta_1 = 0$ with keeping the difference of shape between the positive and the negative regions of $\zeta_1$ and decays to zero [see the transition from Fig. 6(a) to 6(f) and from Fig. 7(a) to 7(f)]. These are true also for other cases.

A comparison with the other cases shows that the function $\Psi^B/((\hat{m}^B)^{3/2} X_0^B)$ is almost independent of $\hat{m}^B$ and $X_0^A$ if it is considered as a function of $\sqrt{\hat{m}^B}\zeta_1$ and $\sqrt{\hat{m}^B}\zeta_\rho$. On the other hand, the function $\Psi^A/X_0^A$ rather depends on $\hat{m}^B$ and $X_0^A$ mainly in $\zeta_1 < 0$ region. The difference between $\zeta_1 > 0$ and $\zeta_1 < 0$ regions is larger for larger $\hat{m}^B$ and for smaller $X_0^A$.

We omit the information about the velocity distribution functions for the diffusion-slip problem because an example of the reduced velocity distribution function has already been shown in Ref. [22]. The qualitative features are the same as those described in the fourth paragraph.

Table II: Coefficient $b_{II}^{(n)}$ $(n = 0, \ldots, N)$ in Eq. (51) for the diffusion-slip coefficient $b_{II}$.

| | $m^B/m^A$ | | | |
|---|---|---|---|---|
| $n$ | 2 (N=8) | 4 (N=12) | 5 (N=12) | 10 (N=16) |
| 0 | 2.49793(−1)* | 6.73235(−1) | 8.66287(−1) | 1.71982 |
| 1 | 5.31606(−2) | 2.55179(−1) | 3.68719(−1) | 9.66600(−1) |
| 2 | 4.27174(−3) | 4.68653(−2) | 8.07502(−2) | 3.14293(−1) |
| 3 | 5.14404(−4) | 1.01504(−2) | 2.00150(−2) | 1.09560(−1) |
| 4 | 4.72189(−5) | 2.12351(−3) | 4.94761(−3) | 3.94440(−2) |
| 5 | 5.62893(−6) | 4.69641(−4) | 1.26793(−3) | 1.45152(−2) |
| 6 | 5.54615(−7) | 1.03165(−4) | 3.27088(−4) | 5.42339(−3) |
| 7 | 6.63470(−8) | 2.31888(−5) | 8.56221(−5) | 2.04847(−3) |
| 8 | 6.74049(−9) | 5.21745(−6) | 2.25515(−5) | 7.80244(−4) |
| 9 | – | 1.18834(−6) | 5.98659(−6) | 2.99082(−4) |
| 10 | – | 2.70543(−7) | 1.60365(−6) | 1.15247(−4) |
| 11 | – | 6.44901(−8) | 4.58402(−7) | 4.46001(−5) |
| 12 | – | 1.42769(−8) | 1.14978(−7) | 1.73405(−5) |
| 13 | – | – | – | 6.77619(−6) |
| 14 | – | – | – | 2.70263(−6) |
| 15 | – | – | – | 1.19130(−6) |
| 16 | – | – | – | 4.12502(−7) |

* Read as $2.49793 \times 10^{-1}$.

Table III: The values of the slip coefficients $b_I$ and $b_{II}$ by the formula (51).

| | $b_I$ | | | | $b_{II}$ | | | |
|---|---|---|---|---|---|---|---|---|
| $X_0^A \setminus m^B/m^A$ | 2 | 4 | 5 | 10 | 2 | 4 | 5 | 10 |
| 0 | 0.4571 | 0.3232 | 0.2891 | 0.2044 | 0.1002 | 0.1141 | 0.1125 | 0.0987 |
| 0.1 | 0.4599 | 0.3199 | 0.2854 | 0.2028 | 0.1098 | 0.1309 | 0.1300 | 0.1155 |
| 0.3 | 0.4731 | 0.3241 | 0.2879 | 0.2054 | 0.1330 | 0.1769 | 0.1794 | 0.1659 |
| 0.5 | 0.4981 | 0.3469 | 0.3082 | 0.2198 | 0.1637 | 0.2514 | 0.2634 | 0.2619 |
| 0.7 | 0.5388 | 0.4007 | 0.3605 | 0.2600 | 0.2059 | 0.3864 | 0.4277 | 0.4871 |
| 0.9 | 0.6023 | 0.5231 | 0.4929 | 0.3937 | 0.2666 | 0.6805 | 0.8365 | 1.311 |
| 1 | 0.6465 | 0.6465 | 0.6465 | 0.6465 | 0.3078 | 0.9882 | 1.3424 | 3.173 |

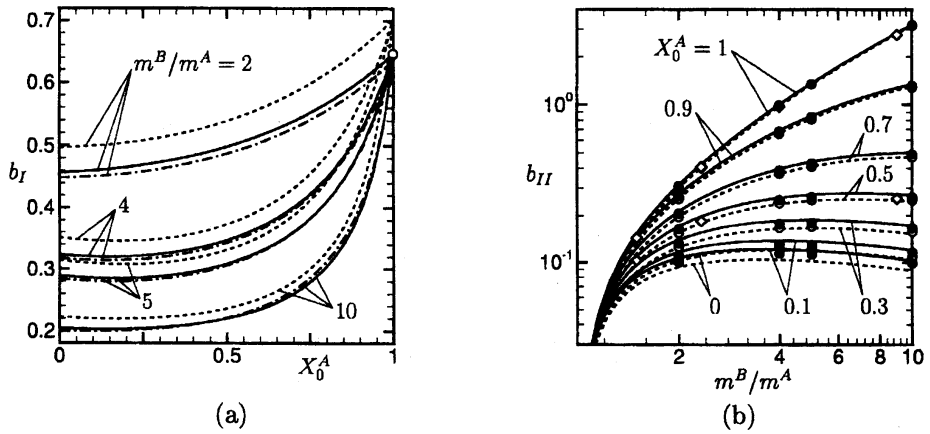


Figure 3: Comparison with the previous results. (a) $b_I$ vs $X_0^A$, (b) $b_{II}$ vs $m^B/m^A$ for $X_0^A = 0, 0.1, 0.3, 0.5, 0.7, 0.9$, and 1. In (a), the solid line indicates the present result, the dashed line the formula in Ref. [20] (ILT1), the dot-dashed line that in Ref. [25] (ILT2), and the open circle the result in Ref. [16]. In (b), the closed circle indicates the present result; the dashed line the formula in Ref. [20] (ILT1); the solid line that in Ref. [25] (ILT2); the open circle the result in Ref. [26] for $X_0^A = 0.1, 0.3, 0.5, 0.7$, and 0.9; and the open diamond that in Ref. [19] for $X_0^A = 0.5$ and 0.99.

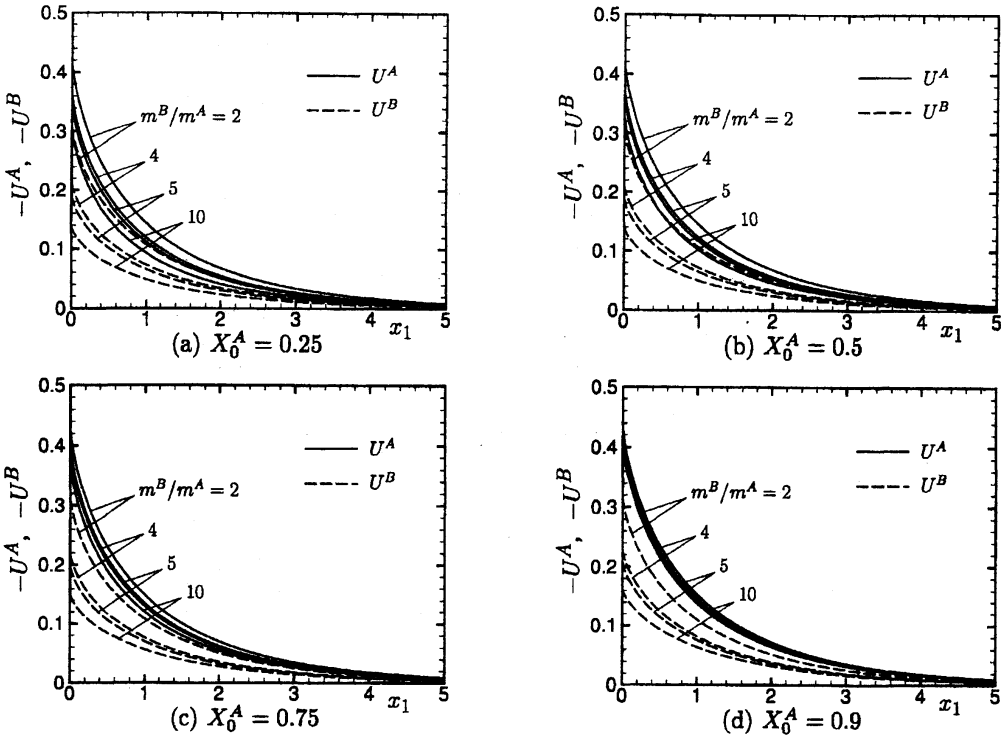


Figure 4: Knudsen-layer functions $U^A$ and $U^B$ for the thermal slip (problem I). (a) $X_0^A = 0.25$, (b) $X_0^A = 0.5$, (c) $X_0^A = 0.75$, and (d) $X_0^A = 0.9$.

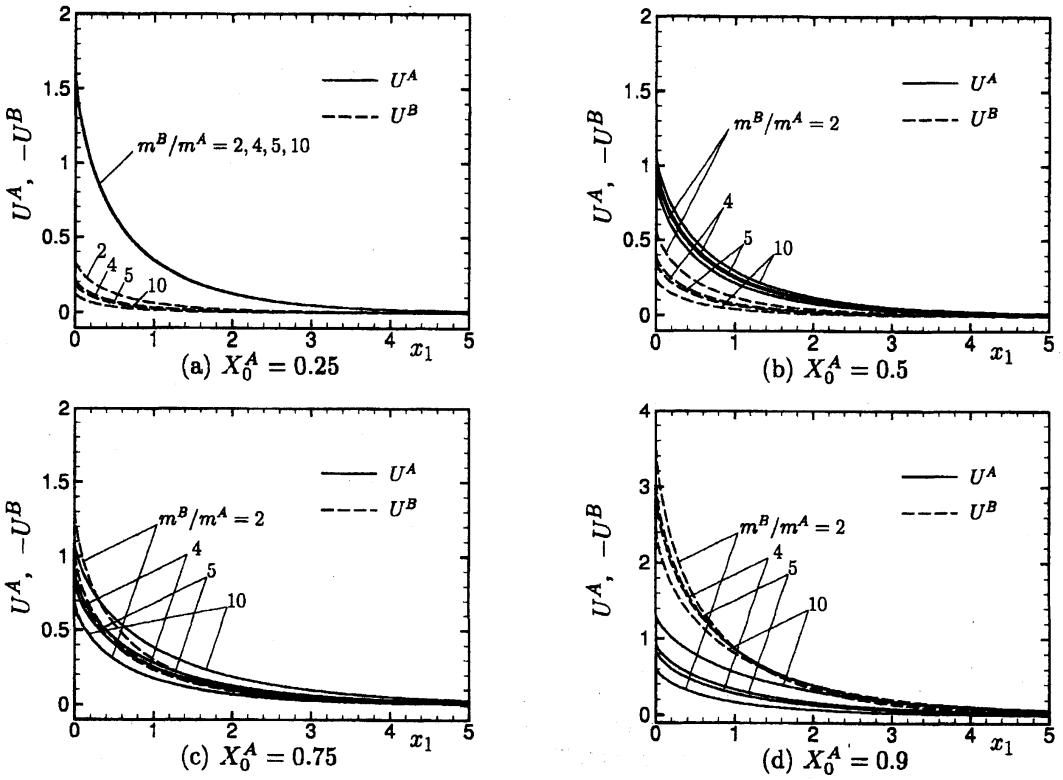


Figure 5: Knudsen-layer functions $U^A$ and $U^B$ for the diffusion slip (problem II). (a) $X_0^A = 0.25$, (b) $X_0^A = 0.5$, (c) $X_0^A = 0.75$, and (d) $X_0^A = 0.9$.

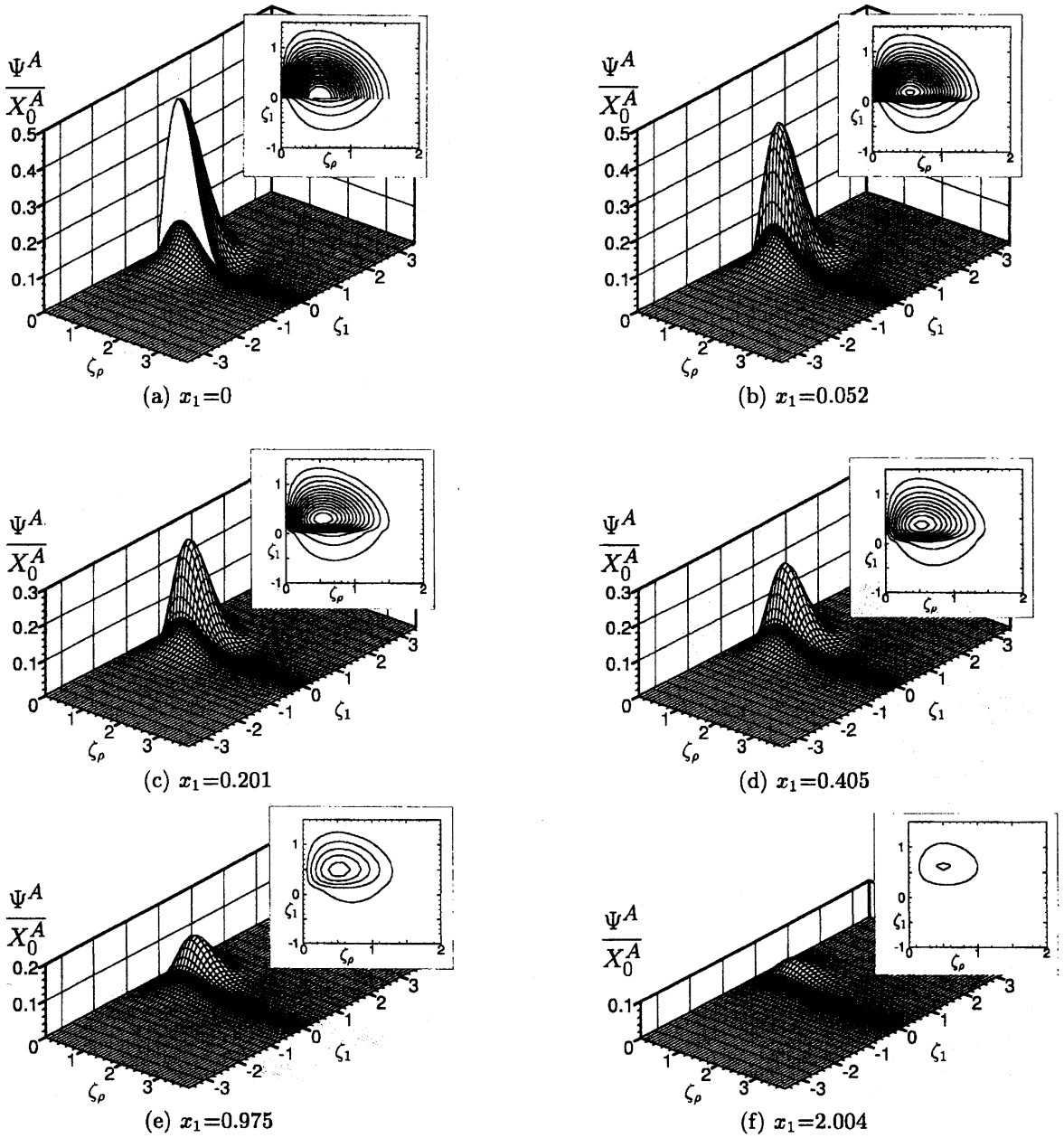


(a) $x_1$=0 (b) $x_1$=0.052

(c) $x_1$=0.201 (d) $x_1$=0.405

(e) $x_1$=0.975 (f) $x_1$=2.004

Figure 6: Reduced velocity distribution function $\Psi^A/X_0^A$ of gas A and its contour plots for the thermal slip (problem I) in the case of $m^B/m^A = 5$ and $X_0^A = 0.5$. (a) $x_1 = 0$, (b) $x_1 = 0.052$, (c) $x_1 = 0.201$, (d) $x_1 = 0.405$, (e) $x_1 = 0.975$, and (f) $x_1 = 2.004$. In the contour plots the curves are drawn with the interval 0.02. The outermost curve indicates the contour $\Psi^A/X_0^A = 0.02$.

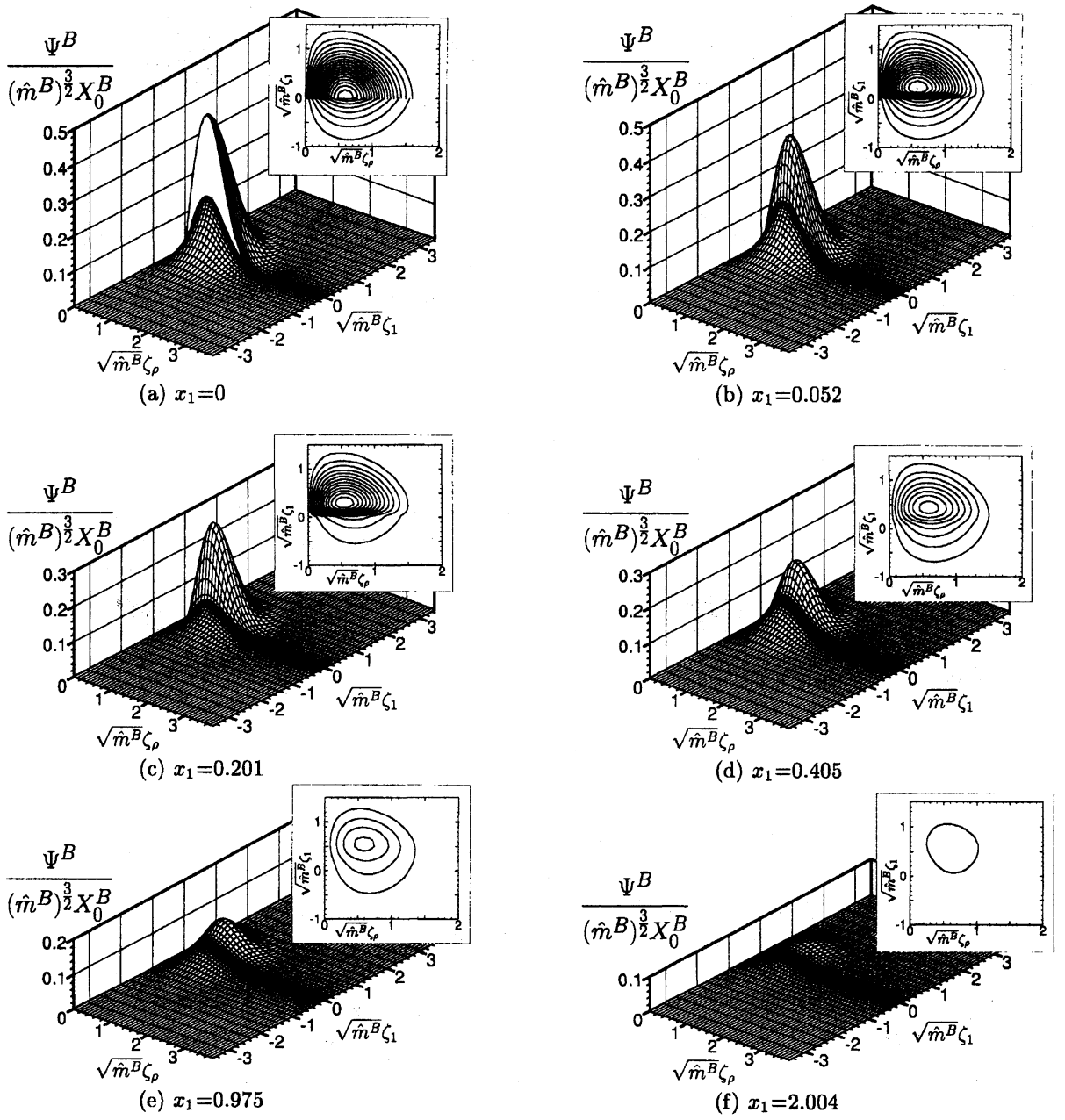


Figure 7: Reduced velocity distribution function $\Psi^B/((\hat{m}^B)^{3/2}X_0^B)$ of gas B and its contour plots for the thermal slip (problem I) in the case of $m^B/m^A = 5$ and $X_0^A = 0.5$. (a) $x_1 = 0$, (b) $x_1 = 0.052$, (c) $x_1 = 0.201$, (d) $x_1 = 0.405$, (e) $x_1 = 0.975$, and (f) $x_1 = 2.004$. See the caption of Fig. 6.

# A Transport Coefficients and Functions $A^\alpha$ and $D^{(\beta)\alpha}$

The coefficients $\hat{\lambda}^{\alpha\prime}$, $\hat{\Delta}_{\alpha\beta}$, $\hat{D}_{T\alpha}$, $\hat{\Gamma}_D^{(\alpha)\beta}$, and $\hat{\lambda}'$ $(\alpha,\beta = A,B)$ are defined by the moments of $A^\alpha$ or $D^{(\beta)\alpha}$ as follows:

$$\begin{gathered}\hat{\lambda}^{\alpha\prime} = \tfrac{5}{2} I_4^\alpha([\hat{m}^\alpha\zeta^2 - \tfrac{5}{2}]A^\alpha), \quad \hat{\Delta}_{\alpha\beta} = \tfrac{5}{2} I_4^\alpha(D^{(\beta)\alpha}), \quad \hat{D}_{T\alpha} = \tfrac{5}{2} I_4^\alpha(A^\alpha), \\ \hat{\Gamma}_D^{(\beta)\alpha} = \tfrac{5}{2} I_4^\alpha([\hat{m}^\alpha\zeta^2 - \tfrac{5}{2}]D^{(\beta)\alpha}), \quad \hat{\lambda}' = X_0^A\hat{\lambda}^{A\prime} + X_0^B\hat{\lambda}^{B\prime},\end{gathered} \tag{52}$$

where

$$I_n^\alpha(F) = \frac{8\pi}{15}\int_0^\infty \zeta^n F E^\alpha d\zeta. \tag{53}$$

Since $\hat{m}^A = \hat{d}^A = 1$ and $X_0^B = 1 - X_0^A$, they are functions of $X_0^A$, $\hat{m}^B$, and $\hat{d}^B$ [see the definitions of $A^\alpha$ and $D^{(\beta)\alpha}$ in Eqs. (9a) and (9b)]. There are some relations among $\hat{\Delta}_{\alpha\beta}$, $\hat{D}_{T\alpha}$, and $\hat{\Gamma}_D^{(\alpha)\beta}$:

$$\begin{gathered}\hat{\Delta}_{\alpha\beta} = \hat{\Delta}_{\beta\alpha}, \quad \hat{D}_{T\alpha} = X_0^A\hat{\Gamma}_D^{(\alpha)A} + X_0^B\hat{\Gamma}_D^{(\alpha)B}, \\ \hat{m}^A X_0^A\hat{\Delta}_{\alpha A} + \hat{m}^B X_0^B\hat{\Delta}_{\alpha B} = 0, \quad \hat{m}^A X_0^A\hat{D}_{TA} + \hat{m}^B X_0^B\hat{D}_{TB} = 0.\end{gathered} \tag{54}$$

The last two relations are the subsidiary conditions for $A^\alpha$ and $D^{(\beta)\alpha}$ [see Eqs. (9a) and (9b)]. The $\hat{\Delta}_{\alpha\beta}$ and $\hat{D}_{T\alpha}$ are directly related to the generalized diffusion coefficient [40] $\Delta_{\alpha\beta}$ and the thermal diffusion coefficient [40] $D_{T\alpha}$ as follows:

$$\Delta_{\alpha\beta} = (\sqrt{\pi}/2)\hat{\Delta}_{\alpha\beta}(2kT_0/m^A)^{1/2}\ell_0, \quad D_{T\alpha} = (\sqrt{\pi}/2)\hat{D}_{T\alpha}(2kT_0/m^A)^{1/2}\ell_0. \tag{55}$$

The reader is referred to the Appendix A in Refs. [54] and [5] for further details.

# B Expression of Integral Kernels

Here we give the explicit expression of $\mathcal{K}_J^{\beta\alpha}$ $(J = 1,2,3)$ in Eq. (22).

$$\mathcal{K}_1^{\beta\alpha} = \begin{cases} \sqrt{\dfrac{2}{\pi}}\left(\dfrac{\hat{\mu}^{\beta\alpha}}{\hat{\mu}^{\beta\alpha}}\right)^2 \xi_\rho \mathcal{J}_1^{\beta\alpha}(\xi_1,\xi_\rho,\zeta_1,\zeta_\rho), & \text{if} \quad \hat{m}^\alpha \neq \hat{m}^\beta, \\ \mathcal{K}_2^{\beta\alpha}, & \text{if} \quad \hat{m}^\alpha = \hat{m}^\beta, \end{cases} \tag{56}$$

$$\mathcal{K}_2^{\beta\alpha} = (\frac{\pi}{2}\hat{m}^\alpha\hat{m}^\beta)^{1/2}(\hat{\mu}^{\beta\alpha})^{-2}\xi_\rho e^{\hat{m}^\alpha|\zeta|^2}\mathcal{J}_2^{\beta\alpha}(\xi_1,\xi_\rho,\zeta_1,\zeta_\rho), \tag{57}$$

$$\mathcal{K}_3^{\beta\alpha} = \frac{\sqrt{2\pi}}{3k}\xi_\rho[(\xi_1-\zeta_1)^2 + (\xi_\rho+\zeta_\rho)^2]^{1/2}[(k-2)E(k) + 2(1-k)F(k)], \tag{58}$$

with

$$\mathcal{J}_1^{\beta\alpha} = \int_0^\pi d\varphi_\xi \cos\varphi_\xi |\boldsymbol{\xi} - \boldsymbol{\zeta}| I_1^{\beta\alpha}(\xi_1,\xi_\rho,\varphi_\xi,\zeta_1,\zeta_\rho), \tag{59}$$

$$\mathcal{J}_2^{\beta\alpha} = \int_0^\pi d\varphi_\xi \frac{\cos\varphi_\xi}{|\boldsymbol{\xi} - \boldsymbol{\zeta}|} I_2^{\beta\alpha}(\xi_1,\xi_\rho,\varphi_\xi,\zeta_1,\zeta_\rho), \tag{60}$$

$$I_1^{\beta\alpha} = e^{-a^{\beta\alpha}}\int_0^1 dt \cosh(-a^{\beta\alpha}t)\int_0^{\pi/2} ds \cosh(b^{\beta\alpha}\sqrt{1-t^2}\sin s), \tag{61}$$

$$I_2^{\beta\alpha} = \exp\left(-\frac{\hat{m}^\beta}{4}(\frac{\hat{m}^\alpha}{\hat{m}^\beta}|\boldsymbol{\xi} - \boldsymbol{\zeta}| + \frac{|\boldsymbol{\zeta}|^2 - |\boldsymbol{\xi}|^2}{|\boldsymbol{\xi} - \boldsymbol{\zeta}|})^2\right), \tag{62}$$

and

$$a^{\beta\alpha} = (\hat{\mu}_-^{\beta\alpha})^2\left(\frac{|\boldsymbol{\xi}|^2}{2\hat{m}^\alpha} + \frac{|\boldsymbol{\zeta}|^2}{2\hat{m}^\beta} - \frac{\boldsymbol{\xi}\cdot\boldsymbol{\zeta}}{\hat{\mu}^{\beta\alpha}}\right), \tag{63}$$

$$b^{\beta\alpha} = -\hat{\mu}_-^{\beta\alpha}|\boldsymbol{\xi}\times\boldsymbol{\zeta}|, \tag{64}$$

$$\hat{\mu}_-^{\beta\alpha} = \frac{2\hat{m}^\beta\hat{m}^\alpha}{\hat{m}^\beta - \hat{m}^\alpha}, \quad \text{for} \quad \hat{m}^\beta \neq \hat{m}^\alpha, \tag{65}$$

$$k = \frac{4\xi_\rho\zeta_\rho}{(\xi_1-\zeta_1)^2 + (\xi_\rho+\zeta_\rho)^2}. \tag{66}$$

The functions $F$ and $E$ in Eq. (58) are, respectively, the complete elliptic integrals of the first and the second kinds [52] defined by

$$F(k) = \int_0^{\pi/2}(1-k\sin^2\theta)^{-1/2}d\theta, \quad E(k) = \int_0^{\pi/2}(1-k\sin^2\theta)^{1/2}d\theta. \tag{67}$$

In the above expressions, the absolute values of vectors and the inner product of $\boldsymbol{\xi}$ and $\boldsymbol{\zeta}$ are expressed in terms of $\zeta_1$, $\zeta_\rho$, $\xi_1$, $\xi_\rho$, and $\varphi_\xi$ as follows:

$$\begin{aligned} &|\boldsymbol{\xi}-\boldsymbol{\zeta}| = (|\boldsymbol{\xi}|^2 + |\boldsymbol{\zeta}|^2 - 2\boldsymbol{\xi}\cdot\boldsymbol{\zeta})^{1/2}, \quad |\boldsymbol{\xi}\times\boldsymbol{\zeta}| = [|\boldsymbol{\xi}|^2|\boldsymbol{\zeta}|^2 - (\boldsymbol{\xi}\cdot\boldsymbol{\zeta})^2]^{1/2}, \\ &|\boldsymbol{\xi}|^2 = \xi_1^2 + \xi_\rho^2, \quad |\boldsymbol{\zeta}|^2 = \zeta_1^2 + \zeta_\rho^2, \quad \boldsymbol{\xi}\cdot\boldsymbol{\zeta} = \xi_1\zeta_1 + \xi_\rho\zeta_\rho\cos\varphi_\xi. \end{aligned} \tag{68}$$

# C Proof of No Diffusion Slip for the Mixture of Identical Molecules

When the molecules of different species are mechanically identical, i.e., $m^B/m^A = d^B/d^A = 1$, $\tilde{L}^{\beta\alpha}$ is reduced to the collision operator for a single-component gas, say $\tilde{L}$, and the relation

$$\sum_{\alpha=A,B} X_0^\alpha[D^{(A)\alpha}(\zeta) - D^{(B)\alpha}(\zeta)] = 0,$$

holds [54]. As a result, by adding Eqs. (12), (13b), and (14) for $\alpha = A$ and those for $\alpha = B$ respectively, one obtains the following boundary-value problem for $\Psi = \Psi^A + \Psi^B$:

$$\zeta_1\frac{\partial\Psi}{\partial x_1} = \tilde{L}(\Psi), \tag{69}$$

$$\Psi = -2\zeta_2 b_{II}, \quad \zeta_1 > 0, \quad x_1 = 0, \tag{70a}$$

$$\Psi \to 0, \quad \text{as} \quad x_1 \to \infty, \tag{70b}$$

where $\tilde{L}(f) = \tilde{L}^{\beta\alpha}(f,f)$ with $\hat{m}^\beta = \hat{m}^\alpha = 1$. This is the Knudsen-layer problem for a single-component gas, and thus there is the theorem for the existence and uniqueness of the solution (see Sec. 3.2). Since the set $\Psi = 0$ and $b_{II} = 0$ is seen to satisfy Eqs. (69)–(70b), $\Psi = 0$ is the unique solution, and the diffusion-slip flow is not induced ($b_{II} = 0$).

# References


[1] Y. Sone, in *Rarefied Gas Dynamics*, edited by L. Trilling and H. Y. Wachman (Academic Press, New York, 1969), Vol. I, p. 243.

[2] Y. Sone, in *Rarefied Gas Dynamics*, edited by D. Dini (Editrice Tecnico Scientifica, Pisa, 1971), Vol. II, p. 737.

[3] Y. Sone, in *Advances in Kinetic Theory and Continuum Mechanics*, edited by R. Gatignol and Soubbaramayer (Springer, Berlin, 1991), p. 19.

[4] Y. Sone, *Kinetic Theory and Fluid Dynamics*, Modeling and Simulation in Science, Engineering and Technology (Birkhäuser, Boston, 2002).

[5] S. Takata and K. Aoki, Transp. Theory Stat. Phys. **30**, 205 (2001); **31**, 289(E) (2002).

[6] Y. Sone, K. Aoki, S. Takata, H. Sugimoto, and A. V. Bobylev, Phys. Fluids **8**, 628 (1996); **8**, 841(E) (1996).

[7] Y. Sone, in *Rarefied Gas Dynamics*, edited by C. Shen (Peking University Press, Beijing, 1997), p. 3.

[8] Y. Sone, Annual Review of Fluid Mechanics **32**, 779 (2000).

[9] E. H. Kennard, *Kinetic Theory of Gases*, (McGraw-Hill, New York, 1938).

[10] H. A. Kramers and J. Kistemaker, Physica **10**, 699 (1943).

[11] Y. Sone, J. Phys. Soc. Jpn. **21**, 1836 (1966).

[12] L. Waldmann and K. H. Schmitt, Z. Naturforschg. **16a**, 1343 (1961).

[13] V. M. Zhdanov, Sov. Phys. Tech. Phys. **12**, 134 (1967).

[14] S. K. Loyalka, Phys. Fluids **14**, 2599 (1971).

[15] Y. Onishi, ZAMP **37**, 573 (1986).

[16] T. Ohwada, Y. Sone, and K. Aoki, Phys. Fluids A **1**, 1588 (1989).

[17] S. K. Loyalka, Phys. Fluids A **1**, 403 (1989).

[18] I. V. Volkov and V. S. Galkin, Fluid Dynamics **25**, 937 (1990).

[19] Yu. I. Yalamov, A. A. Yushkanov, and S. A. Savkov, J. Eng. Phys. Thermophys. **66**, 367 (1994).

[20] I. N. Ivchenko, S. K. Loyalka, and R. V. Tompson, J. Vac. Sci. Technol. A **15**, 2375 (1997).

[21] C. M. Huang, R. V. Tompson, T. K. Ghosh, I. N. Ivchenko, and S. K. Loyalka, Phys. Fluids **11**, 1662 (1999).

[22] S. Takata in *Rarefied Gas Dynamics*, edited by T. J. Bartel and M. A. Gallis (AIP, Melville, 2001), p. 22.

[23] C. E. Siewert, J. Quant. Spectrosc. Radiat. Transf. **75**, 21 (2002).

[24] C. E. Siewert and F. Sharipov, Phys. Fluids **14**, 4123 (2002).

[25] I. N. Ivchenko, S. K. Loyalka, and R. V. Tompson, ZAMP **53**, 58 (2002).

[26] F. Sharipov and D. Kalempa, in *Rarefied Gas Dynamics*, edited by A. D. Ketsdever and E. P. Muntz (AIP, Melville, 2003), p. 164.

[27] Y. Sone, T. Ohwada, and K. Aoki, Phys. Fluids A **1**, 363 (1989).

[28] T. Ohwada, K. Aoki, and Y. Sone, in *Rarefied Gas Dynamics: Theoretical and Computational Techniques*, edited by E. P. Muntz, D. P. Weaver, and D. H. Campbell (AIAA, Washington, DC, 1989), p. 70.

[29] Y. Sone, T. Ohwada, and K. Aoki, Phys. Fluids A **1**, 1398 (1989).

[30] T. Ohwada, Y. Sone, and K. Aoki, Phys. Fluids A **1**, 2042 (1989).

[31] Y. Sone, S. Takata, and T. Ohwada, Eur. J. Mech., B/Fluids **9**, 273 (1990).

[32] Y. Sone, T. Ohwada, and K. Aoki, in *Mathematical Aspects of Fluid and Plasma Dynamics*, Lecture Notes in Mathematics, Vol. 1460, edited by G. Toscani, V. Boffi, and S. Rionero (Springer-Verlag, Berlin, 1991), p. 186.

[33] T. Ohwada and Y. Sone, Eur. J. Mech., B/Fluids **11**, 389 (1992).

[34] S. Takata, Y. Sone, and K. Aoki, Phys. Fluids A **5**, 716 (1993).

[35] S. Takata, K. Aoki, and Y. Sone, in *Rarefied Gas Dynamics: Theory and Simulations*, edited by B. D. Shizgal and D. P. Weaver, Vol. 159 of Progress in Astronautics and Aeronautics (AIAA, Washington, D. C., 1994), p. 626.

[36] Y. Sone, S. Takata, and M. Wakabayashi, Phys. Fluids **6**, 1914 (1994).

[37] S. Takata and Y. Sone, Eur. J. Mech., B/Fluids **14**, 487 (1995).

[38] S. Takata, Y. Sone, D. Lhuillier, and M. Wakabayashi, Computers Math. Applic. **35**, 193 (1998).

[39] M. N. Kogan, *Rarefied Gas Dynamics* (Plenum, New York, 1969).

[40] S. Chapman and T. G. Cowling, *The Mathematical Theory of Non-Uniform Gases*, 3rd Ed. (Cambridge University Press, Cambridge, 1995).

[41] J. O. Hirshfelder, C. F. Curtiss, and R. B. Bird, *Molecular Theory of Gases and Liquids* (John Wiley & Sons, New York, 1954).

[42] S. Takata, S. Yasuda, K. Aoki, and T. Shibata, in *Rarefied Gas Dynamics*, edited by A. D. Ketsdever and E. P. Muntz (AIP, Melville, 2003), p. 106.

[43] K. Aoki, C. Bardos, and S. Takata, J. Stat. Phys. **112**, 629 (2003).

[44] H. Grad, in *Transport Theory*, edited by R. Bellman, G. Birkhoff, and I. Abu-Shumays (AMS, Providence, 1969), p. 269.

[45] N. B. Maslova, *USSR Comp. Math. Phys.* **22**, 208 (1982).

[46] C. Bardos, R. E. Caflisch, and B. Nicolaenko, Commun. Pure Appl. Math. **39**, 323 (1986).

[47] C. Cercignani, in *Trends in Applications of Pure Mathematics to Mechanics*, edited by E. Kröner and K. Kirchgässner (Springer-Verlag, Berlin, 1986), p. 35.

[48] F. Coron, F. Golse, and C. Sulem, Commun. Pure Appl. Math. **41**, 409 (1988).

[49] F. Golse and F. Poupaud, Math. Methods Appl. Sci. **11**, 483 (1989).

[50] H. Grad, in *Rarefied Gas Dynamics,* edited by J. A. Laurmann (Academic Press, New York, 1963), Vol. I, p. 26.

[51] Y. Sone and S. Takata, Transp. Theory Stat. Phys. **21**, 501 (1992).

[52] M. Abramowitz and I. A. Stegun, *Handbook of Mathematical Functions* (Dover, New York, 1968).

[53] C. Gasquet and P. Witomski, *Fourier Analysis and Applications* (Springer, New York, 1999).

[54] S. Takata and K. Aoki, Phys. Fluids **11**, 2743 (1999).

[55] F. J. McCormack, Phys. Fluids **16**, 2095 (1973).